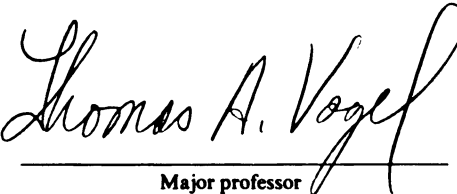This is to certify that the

dissertation entitled

Geochemistry of the Elkhorn Mountains Volcanics,
Southwestern Montana: Implications for the Early
Evolution of a Volcanic-Plutonic Complex

presented by

Carolyn Rutland

has been accepted towards fulfillment
of the requirements for

Doctoral degree in Geology

Major professor

Date 11/7/85

0-12771

GEOCHEMISTRY OF THE ELKHORN MOUNTAINS VOLCANICS, SOUTHWESTERN MONTANA: IMPLICATIONS FOR THE EARLY EVOLUTION OF A VOLCANIC-PLUTONIC COMPLEX

By

Carolyn Rutland

A DISSERTATION

Submitted to
Michigan State University
in partial fulfillment of the requirements
for the degree of

DOCTOR OF PHILOSOPHY

Department of Geological Sciences

1985

ABSTRACT

GEOCHEMISTRY OF THE ELKHORN MOUNTAINS VOLCANICS, SOUTHWESTERN MONTANA: IMPLICATIONS FOR THE EARLY EVOLUTION OF A VOLCANIC-PLUTONIC COMPLEX

By

Carolyn Rutland

The Cretaceous Boulder batholith and Elkhorn Mountains Volcanics, southwestern Montana, are an example of a large volume, volcanic-plutonic association whose level of erosion has exposed the cogenetic intrusive rocks while preserving sizeable portions of the volcanic field. Geochemical studies of the volcanic rocks yield information about the origin, composition, and evolution of the magmas; such conclusions may then be compared to similar information about the crystallized products, represented in the plutonic rocks. Taken together, the volcanic and plutonic rocks provide an improved understanding of the mechanisms influencing the earliest and latest stages of development of a large, complex magmatic system.

Relatively constant Th/Ta and enrichment of Ce, Ta, Hf, Zr, Yb, and Th in a sequence of lava flows and ash-flow sheets in the Elkhorn Mountains Volcanics are consistent with the hypothesis that the sequence is related to evolution of a single magmatic system, envisioned as several separately evolving magma bodies of combined batholithic dimensions. Interpretation of chemical trends within this sequence has shown that 1) some fractionation of olivine influenced the evolution of one group of lava flows, 2) a small amount of fractionation of plagioclase

occurred in the ash-flow sheets, but none in the lava flows, and 3) no fractionation of alkali feldspar occurred. Relationships among the lava flows and ash-flow sheets were not dominated by either crystal-liquid fractionation or magma mixing, but may have been influenced somewhat by a combination of these mechanisms. The absence of zoning in the ash-flow sheets is interpreted as indicating that eruption occurred before development of a highly silicic upper zone in the magma chamber(s).

The Elkhorn Mountains Volcanics are similar to the main series of the cogenetic Boulder batholith in K_2O, Na_2O, CaO, and Rb contents. However, the plutonic phase was influenced more by feldspar fractionation than was the volcanic phase.

From interpretation of Zr abundances and $(Na_2O + K_2O)/Al_2O_3$ in the volcanic rocks, it is considered probable that the parent magma was peralkaline.

Peralkalinity of the parent magma (as an indicator of high K_2O contents) and the relatively high Rb (approximately 35-165 ppm) and Sr (approximately 300-1200 ppm) are evidence for a magmatic source in crust of intermediate thickness above a subduction zone at intermediate depth. This is evidence in support of earlier conclusions (Doe and others, 1968; Tilling, 1973), that the magmas originated in the lower crust or upper mantle. The lack of a significant Eu anomaly in the volcanic rocks, implying that the source region was not in the stability range of feldspar, is consistent with this interpretation.

Shallow level processes are rejected as dominant processes in the evolution of the Elkhorn Mountains Volcanics. Instead, the major chemical characteristics of the magmas could reflect the source(s) of the liquids. Characteristics inherited during magma generation at depth, rather than those acquired during residence at shallow crustal levels, may be typical of similar eruptive units of intermediate SiO_2 range.

ACKNOWLEDGEMENTS

TABLE OF CONTENTS

TABLE OF CONTENTS (continued)

LIST OF FIGURES

LIST OF TABLES

INTRODUCTION

The Cretaceous Boulder batholith and Elkhorn Mountains Volcanics in southwestern Montana are an excellent example of a large volume, volcanic-plutonic association whose level of erosion has exposed the cogenetic intrusive rocks while preserving sizeable portions of the volcanic field. In such a plutonic-volcanic association, the plutonic rocks yield information primarily about the crystallized products and the compositions of the magmas must be inferred. In contrast, the volcanic rocks, which consist primarily of lava flows and ash-flow sheets in the Elkhorn Mountains Volcanics, yield information about the composition of the magmas.

It is well accepted that both ash-flow sheets and calderas are products of violent, rapid evacuations of the upper portions of shallow-level magma chambers (Williams, 1941; Smith, 1960). In this context, a sequence of ash flows preserves quenched magma as ash-flow tuffs from the uppermost part(s) of a magmatic system and hence a partial record of its evolution in time. Lava flows from the same system complement the record of the ash-flow sheets by furnishing samples of magma from other portions of the magmatic system. However, lava flows generally represent much smaller volumes of magma than do ash-flow sheets.

The sources of the ash flows and lava flows of the Elkhorn Mountains Volcanics may have comprised several overlapping calderas and vents. Although each eruptive episode may have tapped its own localized magma chamber, all were probably related to the larger, complex magmatic system, whose final crystallization products were the plutons of the Boulder batholith. The volcanic products of an individual volcanic center or vent would thus largely be determined

by the evolutionary processes operating there, but could also be influenced by events common to the other parts of the overall magmatic system.

In general, each eruptive cycle would begin with a pre-caldera stage dominated by eruptions of lavas and pyroclastic materials, followed by a climactic caldera-forming event with attendant voluminous ash flows. The post-caldera stage would again be a period of less energetic and low-volume eruption of lavas and pyroclastic materials (Christiansen, 1979).

Because the Elkhorn Mountains Volcanics are only the remnants of a huge, complex volcanic field, no single caldera cycle is likely to be preserved completely. However, the intercalated ash-flow sheets and lava flows do record the overall chemical evolution of the larger magmatic system; individual caldera cycles may possibly be identified within these ash-flow sheets and lava flows.

The chemical variation of each successive ash-flow sheet and lava flow reflects the long-term evolution of the system. Possible compositional zoning within the ash-flow sheets is especially significant. The recognition that compositional zoning within ash-flow sheets probably reflects pre-eruption gradients in the magma body (Smith and Bailey, 1966; Lipman and others, 1966) has provided a fundamental basis for many detailed studies of ash flow sheets (cf. Hildreth, 1979; Mahood, 1981; Bacon and others, 1981; Whitney and Stormer, 1985; Leat and others, 1984).

Recent modeling of ash flow eruption dynamics has demonstrated that an ash-flow sheet is not a simple inversion of the pre-eruptive trends (Spera, 1981; Blake, 1981). Nevertheless, the overall chemical pattern in the magma body is generally preserved in the ash-flow sheets (Lipman and others, 1966).

Studies of zoned ash-flow sheets in turn have led to the formulation of models for the evolution of their source chambers (Smith, 1979; Hildreth, 1981).

The nature of the causes of such differentiation is still much debated (Hildreth, 1981; Michael, 1983; Cameron, 1984; Baker and McBirney, 1985).

The development of the cogenetic plutonic rocks may be broadly traced within the same caldera cycles which produced the volcanic materials. The model proposed by Steven and Lipman (1966) for the San Juan volcanic field, Colorado, can likewise be applied to the Elkhorn Mountains Volcanics-Boulder batholith association (Lipman, 1979, 1984). Thus, each cycle of volcanic activity reflects the upward movement of magma, climaxing with the failure of the roof of each particular chamber or cupola of the larger magmatic system and ash flow eruption, and waning as the remaining material crystallized. The chemistry of the plutons of the Boulder batholith offers evidence of the evolutionary processes operating only during the final cooling and crystallization stages. Comparison of the chemical trends of the batholith with those in the ash-flow sheets and lavas contrasts crystallized products (that is, the batholith) and magma (that is, the volcanic rocks). This comparison may contribute to an improved understanding of the mechanisms controlling the earliest and latest development of a large, complex magmatic system.

Accordingly, this investigation of the Elkhorn Mountains Volcanics-Boulder batholith association has the following objectives.

1) To identify the major processes that led to the chemical diversity of the Elkhorn Mountains Volcanics, based on interpretation of the major and trace element variations within the volcanics, and

2) To compare the evolutionary processes inferred from the volcanic rocks with those recorded in the plutonic rocks.

REGIONAL GEOLOGIC SETTING

The Elkhorn Mountain Volcanics-Boulder batholith region lies east of the Idaho batholith within the Helena salient of the frontal Cordilleran fold and thrust belt (Figure 1). The region is dominated by Sevier-style thrusting on the north. However, the southernmost exposures of the volcanics and southern satellite plutons of the batholith are folded and faulted in structures related to Laramide-style deformation of the Rocky Mountain foreland (Schmidt and Hendrix, 1981). These two structural styles developed coevally from Late Cretaceous to late Paleocene time (about 80 to 60 Ma). Eruption of the Elkhorn Mountains Volcanics took place from about 81 to 76 Ma ago, overlapping emplacement of the Boulder batholith from approximately 78 to 68 Ma ago(Tilling and others, 1968).

For much of the past thirty years the Boulder batholith was the subject of research by members of the U.S. Geological Survey (e.g., Knopf, 1957, 1963; Klepper and others, 1957, 1971; Klepper, Ruppel and others, 1971; Klepper and Smedes, 1959; Becraft and others, 1963; Ruppel, 1961, 1963; Smedes, 1962, 1966, 1967; Smedes and others, 1962; Doe and others, 1968; Tilling, 1973, 1974; Tilling and others, 1968; Robinson and others, 1968). A part of the Elkhorn Mountains Volcanics-Boulder batholith complex lies within the proposed Elkhorn Wilderness Study Area, whose economic potential was evaluated jointly by the U.S. Geological Survey and the U.S. Bureau of Mines (1978). A summary follows of the regional igneous relationships as described in these references.

The Elkhorn Mountains Volcanics were intruded by the Boulder batholith and make up its margins and remaining roof (Figure 1). The volcanics discontinuously cover much of the region from the Deer Lodge valley to the Townsend valley and from the Jefferson River north toward Helena (Klepper and others, 1957). They
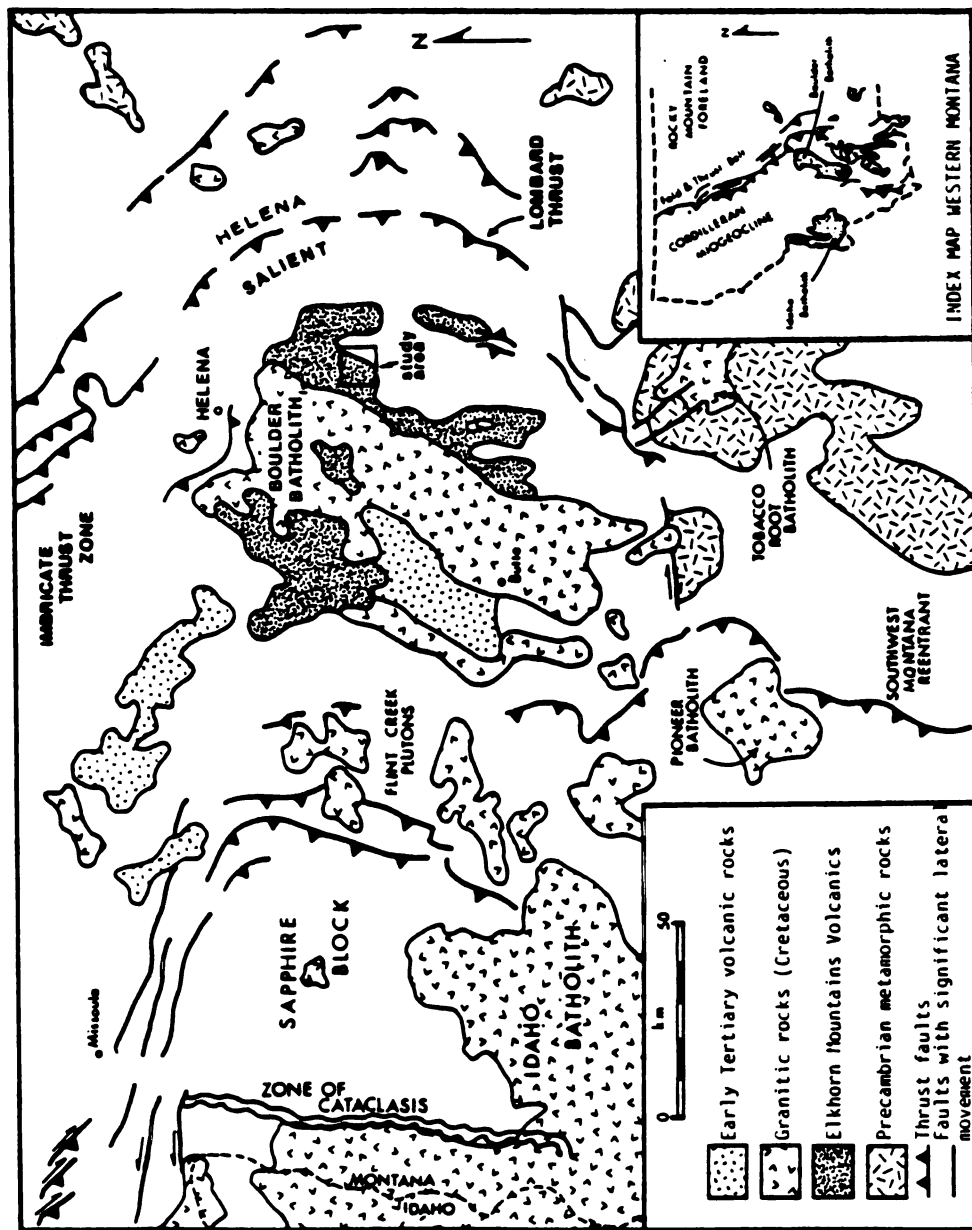
Figure 1. The tectonic setting of the Elkhorn Mountains Volcanics-Boulder batholith region (after Hyndman and others, 1975).

5

are the remnants of an extensive volcanic field that may originally have covered up to 26,000 km^2 and have been at least 3 km and perhaps as much as 4.7 km thick (Klepper and Smedes, 1959; Smedes, 1966). If these estimates are correct, the ash flows in the Elkhorn Mountains Volcanics may have comprised one of the earth's largest known ash flow fields (Smith, 1960a).

Klepper and others (1957) divided the volcanics into three informal members based on their work in the southern Elkhorn Mountains. The lower member consists predominantly of lava flows, autobrecciated lavas, and volcanic sediments, but also contains some thin ash flows; its thickness is as great as 1300 m locally. The middle member, as much as 2290 m thick in places, consists of many layers of ash flows and thin layers of ash-fall sediments. The upper member is composed of water-laid volcanic sediments totalling 630 m. The same lithostratigraphic units of varying thickness have been recognized throughout the region (Klepper, Ruppel and others, 1971; Klepper and others, 1957; Freeman and others, 1958; Nelson, 1963; Smedes, 1966; Becraft and others, 1963; Ruppel, 1961, 1963); however, no correlations of chronological boundaries have been established. There is no formal stratigraphy for the Elkhorn Mountains Volcanics, and usage of the informal division is retained for convenience in referring to the relevant portions of the volcanic pile.

The Boulder batholith is a composite intrusion comprised of at least fifteen epizonal plutons ranging in composition from syenogabbro to alaskite; it is exposed over an area of 6,000 to 7,000 km^2 (Klepper and others, 1971). The batholith is an elongate body of approximately 100 km by 50 km; the largest pluton, the Butte Quartz Monzonite, makes up over 75% of the exposed batholith (Klepper and others, 1971). Estimated thicknesses for the batholith range from less than 5 km (Hamilton and Myers, 1974) to over 15 km (Klepper and others, 1971). Radiometric age dates for the batholith range from approximately 78 to

68 Ma; the Butte Quartz Monzonite was probably emplaced from 76 to 74 Ma ago (Tilling and others, 1968).

Tilling (1973) presented major element chemical and isotopic evidence for recognition of two magma series in the Boulder batholith, the main (or potassic) series and the sodic series. The main series, represented primarily by the plutons in the northern and central parts of the batholith, is characterized by higher K_2O and lower Na_2O contents at any given SiO_2 content. In contrast, the plutons in the southern part of the batholith, most of which comprise the sodic series, contain less K_2O and more Na_2O. The distribution of Rb, Sr, Th, and U, and of lead, oxygen, and hydrogen isotopes among the plutons shows the same two groups (Tilling, 1973, 1977). In a trace element study of the main and sodic series plutons in the southern part of the batholith, Lambe (1981) presented variation diagrams for Nb, Zr, Pb, Cu, and Ba against SiO_2 which also exhibited different patterns in groups of samples representing each magma series.

Collectively, the isotopic data and chemical analyses have been interpreted as indicating a genetic relationship between the Elkhorn Mountains Volcanics and the Boulder batholith, confirming inferences from earlier geologic observations (best summarized by Robinson and others, 1968, but also discussed in Klepper and others, 1957, and Robinson, 1963). Doe and others (1968) concluded that the lead isotopic data for the batholith and the volcanics (represented by only two samples) are compatible with the inferred genetic relationship between them. Tilling (1973, 1974) presented chemical and isotopic evidence comparing the Elkhorn Mountains Volcanics with the main and sodic series of the batholith and concluded that the volcanics are more similar to the "more mafic rocks of the plutonic main series and are distinctly different from any rocks of the sodic series" (Tilling, 1974, p. 1925). The trace element studies of Lambe (1981) are also consistent

7

with a genetic relationship between the Elkhorn Mountains Volcanics and the plutonic main series.

GEOLOGY OF THE STUDY AREA

Much of the preserved remnants of the Elkhorn Mountains Volcanics lies in the region known as the Elkhorn Mountains, located south of Helena, Montana, and north of the Jefferson River between the Missouri and Boulder Rivers (Figure 2). The area around Crow Peak, near the former mining town of Elkhorn in the southern Elkhorn Mountains, was chosen for this project after evaluation of existing geologic reports (specifically, Klepper and others, 1957; Becraft and others, 1963; Smedes, 1962, 1966; Klepper, Ruppel and others, 1971) (Figure 3). W. R. Greenwood (pers. comm., 1981) provided expanded versions of some of the measured sections in these U.S. Geological Survey Professional Papers as well as additional measured sections. After preliminary examination of all available information, the final choice was made by considering a) the relative structural simplicity of the Crow Peak area, b) the availability of good exposures of the volcanics, c) the comparatively mild contact-metamorphic effects of the batholith to the west and the subvolcanic sills and dikes within the area, d) the limited hydrothermal alteration, and e) the accessibility of the area. The study area (Figure 2) is located in the Helena and Deerlodge National Forests in Jefferson County.

Little or no unequivocal physical evidence of the eruptive sources of the primary volcanic materials is preserved at the present level of exposure of the Elkhorn Mountains Volcanics-Boulder batholith complex. However, the structural relationships in the vicinity of the Skyline Mine and the adjacent distribution of a thick welded tuff of the middle member (see Figure 3) may indicate part of the structural rim of a cauldron (U.S.G.S-U.S.B.M. Open File Report 78-325, 1978, p. 67). Specifically, the northwest-trending Skyline fault may be the southern
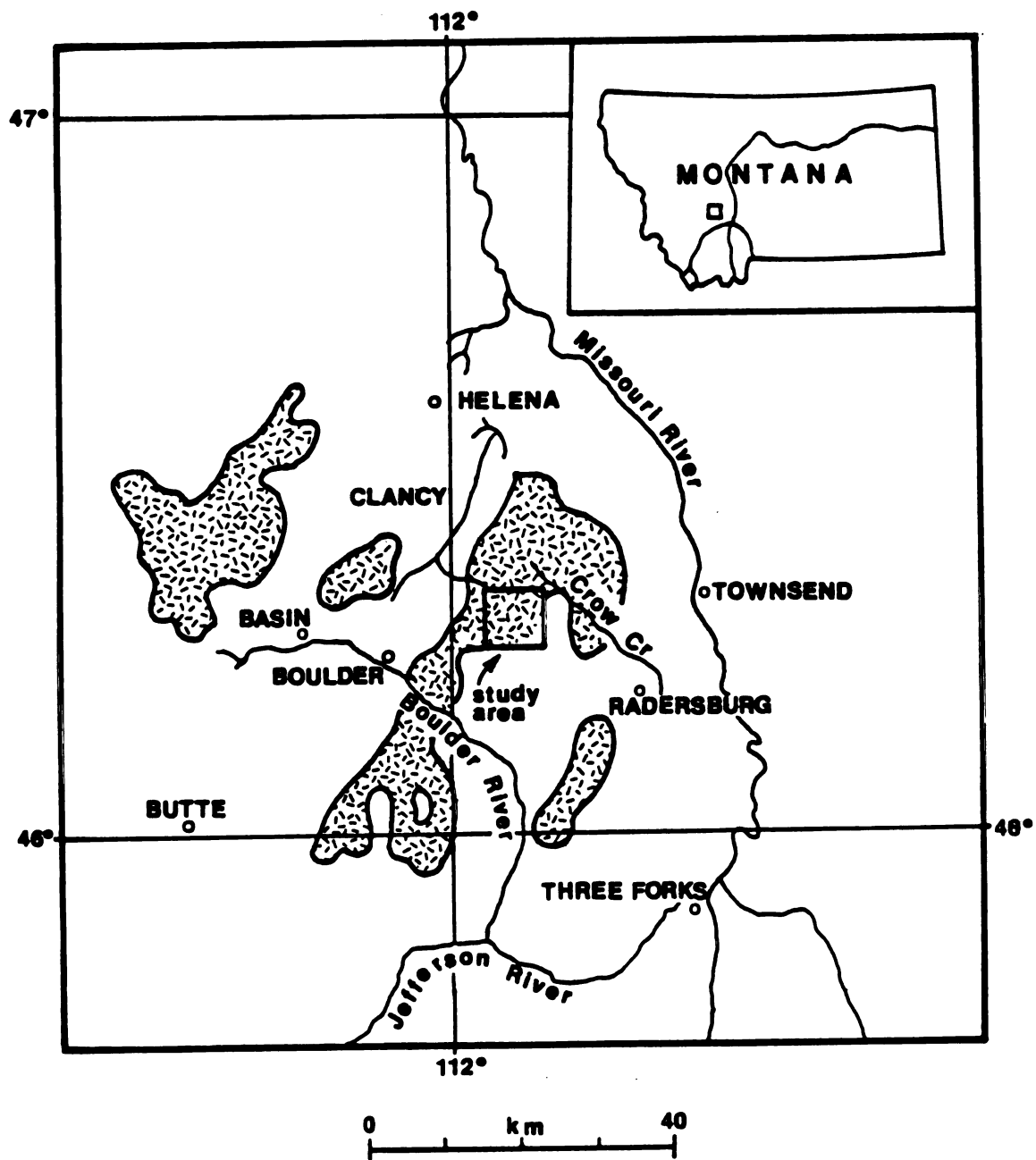
Figure 2. Map of remnants of the Elkhorn Mountains Volcanics in the Elkhorn Mountains; small box indicates study area.
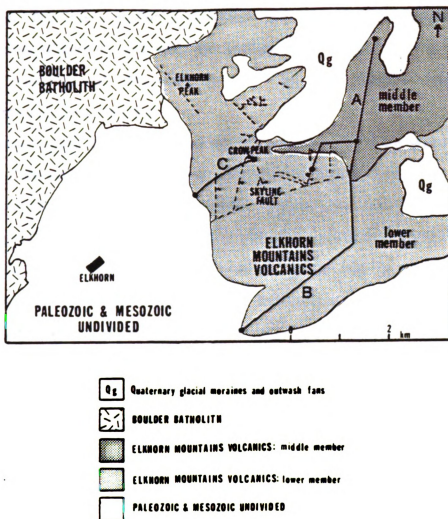
Figure 3. Geologic sketch map of the study area. Traverses labeled A, B, and C indicate the locations of the generalized stratigraphic columns in Figure 4. Dashed lines indicate faults. Modified from Klepper and others (1957).

margin of a structural low within which accumulated intracaldera ash flow accumulated. This interpretation is consistent with the volcanic stratigraphy of the study area (Figure 4), and with the geology and structure of the Elkhorn Mountains volcanics at the northern end of the Elkhorn Mountains (W. R. Greenwood, pers. comm.).

The oldest rocks in the study area are the lower gray to black shales of the Cretaceous Colorado formation, overlain with slight angular unconformity by the Elkhorn Mountains Volcanics. These shales represent the lower part of the Colorado formation; to the east and north on the flanks of the Elkhorn Mountains, complete sections of the Colorado are overlain conformably by the volcanics (Klepper and others, 1957; Klepper, Ruppel and others, 1971; Smedes, 1966). Immediately to the east of the study area, the volcanic sediments of the Slim Sam formation occur between the Colorado (conformably) and the volcanics (locally either conformably or unconformably). The Slim Sam formation consists of erosional debris from the earliest volcanic products; its textural characteristics suggest relatively short transport distances from the source (Klepper and others, 1957).

A fairly thick (about 2065 m) section of the lower and middle members of the Elkhorn Mountains Volcanics is preserved in the study area apparently due to the pre-depositional erosion surface and to post-depositional deformation. Klepper and others (1957) interpreted the unconformity below the volcanics as part of a valley or depression in the Colorado and Slim Sam formations, which allowed a thick accumulation of the volcanics. Subsequent to deposition, folding produced a major syncline whose axis follows the crest of this trough northeastward into the central Elkhorn Mountains (Klepper and others, 1957; Smedes, 1966). Smedes (1966, p. 24) suggested that the pre-volcanic depression might have been a valley formed by erosion along the crest of an older fold.

12

Figure 4. Volcanic stratigraphy of the study area. Column labels A, B, and C correspond to traverse labels in Figure 3. Roman numerals identify units referred to in the text. Letters and Arabic numbers indicate approximate positions of sample sites and correspond to sample numbers in Tables 2 and 3.
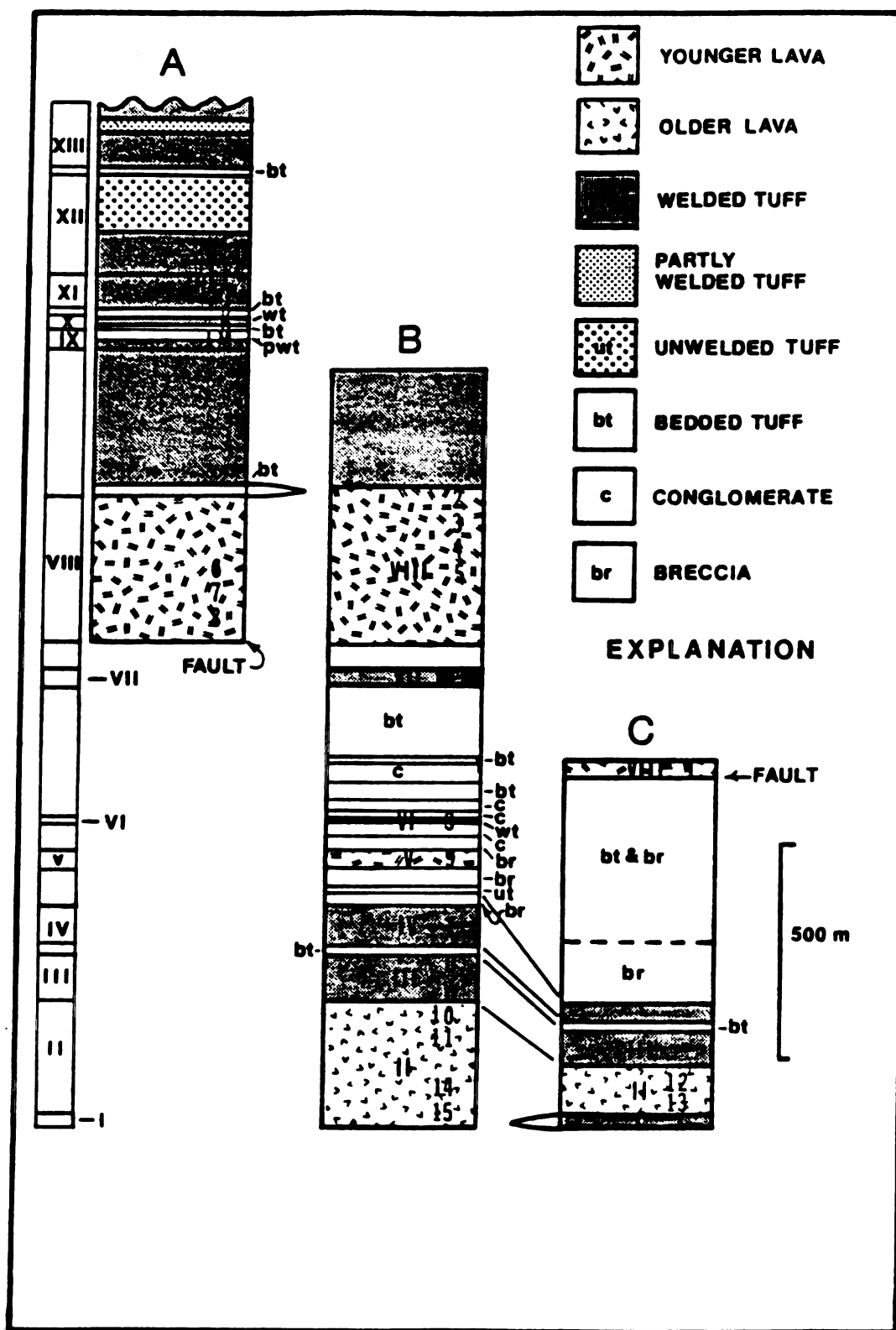
Figure 4.

14

The upper member of the volcanics is not present in the study area.

The salient physical characteristics of several sequences of volcanic lithologies in the lower and middle members of the Elkhorn Mountains Volcanics found in the study area are summarized below. The sequence is illustrated in Figure 4, annotated with Roman numerals to correspond to the following description of the units within the sampled section.

The ash-flow sheets and lava flows in both the lower and middle members contain lithic fragments. In the field, two categories of lithic fragments can be determined, one of xenoliths that are clearly of volcanic origin, generally because of porphyritic textures, and one of xenoliths of ambiguous origin, because they are homogeneous and extremely fine-grained. These latter resemble chips of chert, like that present in the Colorado formation. However, they could also be lithic fragments of aphanitic volcanic rock or of bedded or ash-fall tuff.

Field Characteristics

Lower Member. The lower member of the volcanics is dominated by lava flows (II, ranging in thickness from about 95 m to 252 m; V, about 37 m thick; and VIII, about 348 m thick). The lower member also contains five ash-flow sheets, some of which are associated with underlying ash-fall tuffs, ranging in thickness from about 3 m to 88 m. The remainder of the approximately 1290 m of the lower member is characterized by epiclastic (volcanoclastic) sediments, comprising breccias and conglomerates and their finer-grained equivalents (Figure 4). Some of these layers are clearly waterlain, as evidenced by, for example, graded bedding and channel-fill lenses. A pyroclastic origin is suggested for the others, particularly the finer-grained units immediately underlying ash-flow sheets.

Unit II consists of at least three separate flows which are locally autobrecciated and/or amygdaloidal. The oldest of these is characterized by abundant oatmeal-flake-sized (.5 cm diameter) plagioclase and occasional

hornblende phenocrysts in an aphanitic grey groundmass. This flow is overlain by one containing less coarse plagioclase and more abundant hornblende phenocrysts in a similar matrix. A few lithic fragments and broken plagioclase crystals can be observed in outcrops of both flows. The other flow(s) is laterally discontinuous, whereas the lower two are distinctive, continuous stratigraphic markers.

Unit V is approximately 37.5 m thick (Figure 4). The texture of its lowermost 4.7 meters is almost aphanitic with very small plagioclase crystals and contains abundant lithic fragments. This massive basal layer grades upward into autobrecciated lava for the remaining thickness.

The lava flows in unit VIII are lithologically similar containing, phenocrysts of pyroxene and plagioclase in a vesicular, nearly aphanitic matrix. Locally amygdaloidal, these lava flows are interbedded with thin ash-fall tuffs.

Cooling units cannot be recognized in the ash-flow sheets in the lower member because of post-depositional alteration. However, separate lithologic and textural units within the preserved sheets can be recognized; most of these can be traced laterally throughout the study area. The welded tuffs are the most easily recognized portions of the ash-flow sheets, exhibiting typical textures such as well-developed eutaxitic structures.

The oldest ash-flow sheet (I) is also the basal unit of the Elkhorn Mountains Volcanics in the study area (see Figure 4). The exposures of this unit consist of highly welded tuffs, with fiamme ranging in size from about 1 cm to about 15 cm in length, surrounded by abundant broken plagioclase crystals and mainly andesitic lithic fragments. The exposures in the next ash-flow sheet (III), which overlies the older lava group (see Figure 4), have large fiamme (up to 20 cm in length) and sparse lithic fragments. The matrix is rich in plagioclase; crystal-fragment abundance is uniform throughout the unit. Above this unit is a lapilli tuff which is interpreted as part of the next overlying ash-flow sheet (IV). The fiamme in the

16

welded tuff in this sheet decrease in size from the highest exposures of the unit to the lowest. The matrix in the upper portion contains up to 20% plagioclase crystal fragments, which decrease to less than 5% in the lower portion. Likewise, angular lithic clasts up to about 8 cm in diameter are more abundant in the upper half of the unit than in the lower. Within the primarily epiclastic/pyroclastic sequence in the middle of the lower member (see Figure 4) is another welded tuff (VI), which is inferred to be an erosional remnant of a thicker ash-flow sheet. This interpretation is based on the fact that the unit is welded throughout its 4.7 m thickness and is lacking in non- or partly-welded zones. Just below the lavas of unit VIII the youngest ash-flow sheet (VII) in the lower member. Fiamme are most abundant in the middle 32 m of exposures of this unit, lithic fragments are scarce in its upper 7-8 m, and plagioclase is abundant in the matrix throughout its thickness.

Middle Member. The contact between the middle and lower members in the study area may be disconformable (Klepper and others, 1957); this interpretation is supported by the discontinuous presence of a mostly bedded tuff overlying the younger group of lava flows in the lower member.

The middle member consists of more than 700 meters of ash-flow sheets. The lowermost continuous lithologic unit in the middle member is about 284 m of lithic-rich welded tuff (see Figure 4). This distinctive unit is overlain by another 447 m of variably welded tuffs, ranging from 0.6 m to 110 m in thickness and alternating with ash fall tuffs, some of which show features of reworking. The remainder of the middle member is covered by glacial sediments and recent soils north of the study area. It is not possible to subdivide this sequence into cooling units on the basis of textures and field relationships, although the presence of a devitrified vitrophyre approximately midway through the exposure demonstrates a

cooling break, as do the several well-bedded ash-fall tuffs in the sequence. Therefore, the divisions illustrated in Figure 4 are purely lithologic.

Unit VIII and the lower part of the middle member are cut by a pyroxene porphyry dike of probable andesitic composition. It is likely that this intrusion is similar in age to the volcanics, albeit somewhat younger. Although Klepper and others (1957) describe other intrusions in the study area, none are of mappable size. At least one of these was found on re-examination to be a lava flow (this work; W. R. Greenwood, pers. comm.).

Summary of Thin Section Descriptions

The important microscopic characteristics of the major volcanic units in the stratigraphic sequence in the study area are summarized in the following section as a supplement to the field descriptions and as background for the geochemistry of the volcanics.

Some textural and mineralogical features are common to the ash-flow sheets and the lava flows. Both rock types have been contact-metamorphosed in the aureole of the Boulder batholith. In the ash-flow sheets many primary characteristics have been modified by devitrification and recrystallization, yet their general features remain recognizable as characteristic of ash-flow sheets (summarized by Ross and Smith, 1961). The alteration processes resulted in many similarities between different rock types, and the cause of a particular characteristic cannot always be identified.

There is no primary glass in any of the volcanics, but relict devitrified shards and fiamme remain. The fiamme are now composed mainly of chlorite and epidote, and the formerly glassy groundmass of the ash-flow sheets is generally a very fine-grained mosaic of quartz and feldspar, with minor amounts of epidote, chlorite, and calcite.

In all of the rocks, the plagioclase is partly altered to epidote and/or calcite. The biotite is non-uniform in color, faded from brown to very pale yellow; it contains abundant opaque inclusions. The primary mafic minerals have been altered; in some samples, calcite and other minerals occupy the relict mineral shape.

Because most of the ash-flow sheet samples are from the welded portions of the sheets, they exhibit similar textural characteristics. Ubiquitous eutaxitic structure is distorted around crystal and lithic fragments to varying degrees in all but a few samples. Most samples also contain flattened shard shapes.

The most common lithic fragments in the ash-flow sheets and lava flows are porphyritic. In some samples, more than one porphyritic type can be observed. Lithic fragments of welded tuff are sometimes present. Other lithic fragments are apparently either chert or very fine-grained tuff.

In contrast to the similarities in petrographic characteristics discussed above, the descriptions below are summaries of the distinguishing characteristics observed in thin sections of the ash-flow sheets and lava flows. The Roman numerals in the text correspond to those in Figure 4. Qualitative estimates of mineral percentages are given for the lava flows. Plagioclase compositions have not been determined because most of the plagioclase crystals have been subjected to some form of secondary alteration, such as replacement by calcite or fine-grained material.

I. Ash-flow sheet: The fiamme are a rusty red-brown color and contain phenocrysts of plagioclase and biotite. The plagioclase contains abundant acicular inclusions of apatite. The matrix consists of broken and euhedral plagioclase phenocrysts, as well as biotite, in an intergrowth of quartz, feldspars, epidote, and chlorote. The groundmass also contains amygdules and patches of calcite. Some of the amygdules are dominated by quartz intergrowths. There are three main

19

types of lithic fragments, one probable lava flow, aphanitic with extremely small plagioclase laths, and a second similar type, coarser-grained with plagioclase and K-feldspar. The third lithic fragment type is very fine-grained and may be of sedimentary or volcanic origin.

II. Older lava flow group: The lowermost flow in this group is characterized petrographically by abundant plagioclase phenocrysts (about 40%), hornblende (less than 5%), and clinopyroxene (5-10%), and opaques (about 10%) in a green-brown matrix of chlorite, epidote, calcite, and very small opaques. The overlying lava flow is dominated by large, sieve-textured plagioclase phenocrysts (about 50%) and lesser amounts of clinopyroxene (about 10%), hornblende, and opaques (both 5-10%), again in a green-brown matrix of chlorite, epidote, calcite, and very small opaques. The pyroxene and hornblende are both partly altered, especially around their margins, with opaques concentrated along cleavages and fractures. Many of the plagioclase laths are broken.

III. Ash-flow sheet: The fiamme contain plagioclase and opaque phenocrysts. Some of the largest fiamme are streaky and patchy in grey and green colors, which may reflect the present state of preservation of mixed pumice. The gray-green matrix of chlorite/epidote and quartz and feldspar intergrowth likewise contains plagioclase and opaque phenocrysts. No lithic fragments are obvious in outcrop, but in thin section at least three types are ssen, a lava flow containing fine-grained plagioclase laths, a possibly sedimentary type dominated by minute quartz grains, and fragments of welded ash-flow tuff.

IV. Ash-flow sheet: The fiamme consist of chlorite and epidote and are phenocryst-poor, containing only an occasional plagioclase lath. The gray-brown matrix of chlorite/epidote, opaques, quartz, and feldspar also contains plagioclase phenocrysts, most of which are broken. Several types of lithic fragments are present, including angular pieces of plagioclase porphyry similar to the lava flows

in II. A second probable lava flow type contains abundant hornblende crystals. Fragments of welded ash-flow tuff are present as well.

V. This plagioclase porphyry also contains phenocrysts of clinopyroxene (about 10%) and biotite (less than 5%) in a very dark matrix of biotite, opaques, epidote, chlorite, quartz, and calcite.

VI. Ash-flow sheet: The fiamme contain no phenocrysts. Plagioclase phenocrysts are present in a greenish matrix dominated by chlorite and epidote. Lithic fragments of earlier lava flows and welded ash-flow tuffs dominate the groundmass.

VII. Ash-flow sheet: The fiamme occasionally contain plagioclase phenocrysts, but are mainly phenocryst-free. Plagioclase and rare K-feldspar and biotite are present in the matrix, which consists of opaques, quartz and feldspars. Lithic fragments are of two main types, plagioclase porphyries and welded tuffs.

VIII. Younger lava flow group: The lava flows of this group are all clinopyroxene porphyries, containing 15-20% pyroxene. Less abundant phenocrysts of olivine (about 5%), plagioclase (about 5%), and opaques (5-10%) are also present. The groundmass is composed of felty plagioclase and pyroxene and is sprinkled with opaques. The olivine crystals are rimmed with pyroxene.

Between the units numbered VIII and IX are about 284 meters of lithic-rich welded tuff. Samples from this stratigraphic interval were not submitted for chemical analysis because of the abundance of lithic fragments. Microscopically, the unit contains epidote-rich, phenocryst-free fiamme. The devitrified matrix contains plagioclase and alkali-feldspar crystals and fragments, vugs filled with calcite, quartz, and feldspar intergrowths, and a variety of rock fragments.

IX. Ash-flow sheet: The lower part of this sheet is distinguished by reddish color and by dark, wavy laminations. These thinly laminated bands are concentrations of oxidized opaques and quartz. The degree of distortion and

stretching has apparently destroyed all former shard shapes in this portion of the sheet. The upper part of the unit contains fiamme rich in K-feldspar and quartz. Phenocrysts in the groundmass include plagioclase, K-feldspar, biotite, opaques, and extremely murky pyroxene; the groundmass itself is composed of aggregates of these minerals dominated by quartz and feldspar. Distortions in the groundmass around phenocrysts and fragments indicate the former presence of flattened shards in the matrix. This unit is virtually lithic-free, except for an occasional fragment porphyry or welded tuff.

X. Ash-flow sheet: The fiamme are composed of chlorite, with crystals of K-feldspar and opaques. The major phenocryst in the matrix is plagioclase; the remainder of the matrix consists of intergrown quartz, opaques, biotite, and K-feldspar. The lithic inclusions in this unit are again plagioclase porphyry and welded tuff.

Between units X and XI is another lithic-rich, partly welded tuff unit, which most likely is the base of another ash-flow sheet, because it overlies a thin ashfall tuff; the contact between the two is reworked. In thin section, rocks of this unit show a very fine-grained greyish-green matrix of chlorite and epidote containing crystals and fragments of plagioclase, K-feldspar, and opaques. The fiamme are composed of chlorite and epidote.

XI. Ash-flow sheet: The base of this sheet was probably originally a vitrophyre, as suggested by the squashed and deformed shard shapes in the matrix. Approximately 15% broken and zoned plagioclase crystals are present, as well as opaques and minor amounts of biotite. Above the base the sheet is highly welded tuff, with K-feldspar and strongly altered plagioclase (to calcite) crystals and pieces amongst the deformed shards. Spherulites are also present. The unit contains lithic inclusions of plagioclase porphyry and welded tuff, whose

abundances increase upward in the section; the uppermost portion of the sheet is too lithic-rich for representative sampling and chemical characterization.

XII. Ash-flow sheet: The fiamme in this unit are relatively small and consist of chlorite and opaques. Distortions in the matrix texture indicate the strongly welded nature of the rocks, although individual shards are rarely discernable. Plagioclase and K-feldspar are the dominant phenocrysts in the matrix of quartz, feldspar, biotite, chlorite, and epidote. The unit contains very few lithic inclusions.

XIII. Ash-flow sheet: The base of this sheet is highly welded; the fiamme, composed of chlorite and epidote, are few and lack phenocrysts. The matrix consists of a quartz, feldspar, chlorite, epidote intergrowth containing plagioclase and K-feldspar phenocrysts, as well as opaques and occasional hornblende. A few lithic fragments are present and increase upward through the sheet.

Approximately 116 meters of ash-flow sheet material are exposed above the base of ash-flow sheet XIII before glacial deposits cover the remainder of the middle member. This highest exposed portion of the volcanic section is particularly altered, presumably because of the gold, silver, copper, and lead mineralization (U.S.G.S.-U.S.B.M. Open-file Report 78-325, 1978) in the vicinity of the Ballard Mine. For this reason, no samples higher than the base of ash-flow sheet XIII were chemically analysed. No details of their petrography are noteworthy, but all samples show the textural characteristics of welded ash-flow tuffs.

SAMPLING AND ANALYTICAL METHODS

All of the lava flows, the ash-flow sheets, and the possible ash fall units immediately below welded tuffs were sampled. Thus, sampling included a) lavas that represent vent and fissure eruptions of small volume that may have originated from any depth within the magma chamber(s), and b) pyroclastics that represent much more voluminous, caldera-forming evacuations of the upper levels of the magma chamber(s). Large-volume pyroclastic eruptions may form calderas and potentially could provide evidence of any zoning present in the magma chamber(s) prior to such an eruption. An ash fall unit below a welded tuff could preserve the most highly differentiated top of the magma, if both were the product of the same ash-flow eruption.

Alteration of samples must be considered in any geologic sampling scheme and was a particularly acute problem in this project. All of the samples show some contact metamorphic effects associated with the intrusion of the Boulder batholith, although the location of the study area was chosen in part to minimize post-eruption alteration processes. The maximum metamorphic facies seen in this section of the volcanics is lower greenschist; typical mineral assemblages include epidote and chlorite. In the lava flows the olivine and pyroxene crystals are commonly badly altered and the plagioclase cores may be replaced by calcite. Amygdaloidal outcrops were avoided. The ash-flow sheet samples present the greatest difficulties because even under the best of circumstances secondary alteration processes such as devitrification, vapor-phase processes, and hydration may strongly affect the rock chemistry. Samples from the welded parts of the sheets should theoretically show minimal effects of these processes because of their low porosity relative to unwelded parts of the ash flow. Exposures

24

exhibiting obvious evidence of secondary alteration (e.g., lithophysae) were avoided as a matter of course. The age of the Elkhorn Mountains Volcanics proscribes any preserved glass, although evidence of glassy textures remains. Despite the care used in sampling, it would be naive to suggest that no effects of thermal metamorphism or secondary alteration occur in the rocks, and the chemical analyses must be evaluated with these qualifications in mind. Furthermore, the sampling approach introduced some biases into the chemical trends through the stratigraphic section, because no unwelded tuff and very little partly welded tuff were sampled.

In the laboratory, further winnowing resulted from elimination of all samples containing abundant lithic fragments. Where necessary, lithic fragments and amygdules were cut out of selected samples before grinding. It was not possible to remove fiamme physically from the welded tuffs, and bulk rock samples were used. Most samples were crushed and ground between porcelain plates and in an agate mortar; however, some samples were crushed between stainless steel plates and this is believed to have caused spurious Cr results. Welded tuffs containing secondary calcite were leached with glacial acetic acid and sodium acetate.

Major element and selected trace element abundances in the lava flows were determined by inductively coupled plasma emission methods (ICP) at Barringer Magenta, Ltd., Toronto. Other trace elements contained in the lavas, including the rare earth elements, were measured by instrumental neutron activation analysis (INAA) at Lawrence Livermore National Laboratory. The ash-flow samples were analyzed for major elements and for selected trace elements by ICP and for trace elements by INAA at the U.S. Geological Survey, Reston.

Estimates of accuracy were obtained from analyses of standards (Table 1). The fact that Barringer Magenta, Ltd., LLNL, and the U.S.G.S. labs obtain analytical results that agree well with accepted international standards can be interpreted as indicating that inter-laboratory differences have not contributed significantly to compositional differences between the sample groups.

Table 1. Estimates of analytical accuracy.

	BIR-1[2]	ICP	% Diff.	BHVO-1[3]	ICP	% Diff.	RGM-1[3]	ICP	% Diff.	G-2[2]	ICP	% Diff.	GSP-1[1]	ICP	% Diff.
A. SiO_2	47.96	47.8	.33	49.9	49.0	1.8	73.67	73.3	.23	69.11	69.0	.16	67.31	67.7	-0.58
Al_2O_3	15.33	16.0	-3.0	13.85	14.0	-1.1	13.80	13.9	-.72	15.4	15.8	-2.6	15.19	15.2	-0.07
Fe_2O_3	2.06	2.2	-6.8	2.7	2.0	25.9	2.0	1.95	2.5	2.75	2.9	-5.4	4.33 $Fe_2O_{3(T)}$	4.23	2.31
CaO	13.32	13.4	-.6	11.3	11.5	-1.8	1.15	1.4	-21.7	1.94	2.1	-8.2	2.02	2.05	-1.49
MgO	9.7	9.8	-1.0	7.31	7.8	-6.7	.28	.40	-42.9	.76	.83	-9.2	.96	1.07	-11.46
Na_2O	1.82	1.9	-.04	2.29	2.5	-9.2	4.12	4.0	2.9	4.07	4.3	-5.6	2.80	2.96	-5.71
K_2O	.03	.02	33.3	.54	.55	-1.8	4.35	4.3	1.1	4.51	4.6	-2.0	5.53	5.06	8.50
MnO	.17	.17	0	.17	.19	-11.8	.04	.05	-25	.03	.07	-1.3	.04	.0389	2.75
TiO_2													.66	.591	10.45
P_2O_5													.28	.35	-25.00
C. FeO	8.36	8.28	.72	8.55	8.51	.47									
D. TiO_2	.96	.94	2.1	2.69	2.7	-.37	.27	.30	-11.1	.5	.49	2.0			
P_2O_5	.02	.04	-50	.28	.35	-20	.05	.05	0	.16	.17	-21.4			

B. (GSP-1 column)

	AGV-1[3]	INAA	% Diff.	BCR-1[3]	INAA	% Diff.	G-2[3]	INAA	% Diff.	GSP-1[3]	INAA	% Diff.	BCR-1[3]	INAA	% Diff.
E. Ba	1200	1255	-4.58	680	717	-5.4	1900	1890	.52	1300	1280	1.5	680	644	5.3
Co	16	15.5	3.12	36	35.5	1.4	5	4.32	13.6	7.8	6.31	19.1	36	39.89	-9.7
Cr	10	9.5	5.0	15	11.3	24.7	8	6.9	13.75	12	10.0	16.7	15	16.62	-10.8
Cs	1.3	1.21	6.9	0.96	.97	-1.0	1.4	1.36	2.9	1	0.90	10.0	.96	.9761	-1.7
Hf	5	5.08	-1.6	5	4.56	8.8	8	8.04	-.5	14	14.4	-2.9	5	5.448	-9.0
Rb	67	71	-6.0	47	49	-4.2	170	167	1.8	250	248	.8	47	54.05	-15.0
Sb	4.3	4.59	-6.7	0.6	.6	-	0.06	n.d	-	3.1	3.21	-3.5	.6	.7073	-17.88
Sc	12.5	12.0	4.0	33	31.2	5.4	3.5	3.83	2.0	6.6	5.63	14.7	34	34	-.30
Ta	1.4	.98	30.0	0.8	.85	-6.2	0.8	.88	-10.0	1	1.00	0	.8	0.774	3.2
Th	6.4	6.45	-7.8	6.1	6.0	1.6	25	25.0	0	105	102	2.9	6.1	5.763	5.5
U	1.95	1.75	10.3	1.7	1.62	4.7	2.1	1.78	15.2	2.1	2.05	2.4	1.7	1.919	-12.9
Zn	86	92	-7.0	125	129	-3.2	84	83	1.2	105	91	13.3	125	178.5	-42.7
Zr	230	218	9.6	185	200	.5	300	327	-9.0	500	580	-8.0	185	168.5	8.9
La	36	40.4	-12.2	27	26.1	3.3	92	91.3	.76	195	179	8.2	27	27.01	-0.3

F. (BCR-1 column)

Table 1 (continued).

	AGV-1[3]	INAA	% Diff.	BCR-1[3]	INAA	% Diff.	G-2[3]	INAA	% Diff.	GSP-1[3]	INAA	% Diff. F.	BCR-1[3]	INAA	% Diff.
E.															
Ce	71	66.3	6.6	53	50.2	5.3	160	153	4.4	360	403	-11.9	53	53.62	-1.2
Sm	5.9	6.03	-2.2	6.5	5.92	-6.5	7.2	7.33	-1.8	25	25.9	-3.6	6.5	6.411	1.4
Eu	1.6	1.56	2.5	2.0	1.84	8.0	1.4	1.28	8.6	2.4	2.10	12.5	2.0	1.983	.8
Tb	0.7	.7	0	1.0	.88	12.0	0.5	0.43	14.0	1.4	n.d	-	1.0	.9641	3.6
Yb	1.9	1.54	18.95	3.5	3.2	5.9	0.86	0.78	9.3	1.9	1.88	10.5	3.4	3.603	-5.9
Lu	0.3	.24	20.0	0.5	.51	-2.0	0.1	0.10	0	0.2	0.212	-6.0	.52	.4921	3.5

	BCR-1[2]	ICP	% Diff.	BCR-1[3]	INAA	% Diff.				GSP-1[1]	ICP	% Diff.
G.												
Ba	675	660	2.2	800	820	-2.5				1300	1220	6.15
Sr	330	310	6.1	100	100	0				230	247	-7.39
Y	37	30	18.9	25	20	20				Not available		
Zr	190	200	-5.3							Not available		

	BCR-1[2]	AA	% Diff.	RGM-1[3]	AA	% Diff.				GSP-1[1]	ICP	% Diff.
H.												
Co	35	25	28.6	2.3	1.7	26.1				9	10	-11.11
Cr	17.6	15	14.8	4	6.2	-55						
Ni	15.4	13.4	30.0	6	-	-						
V	399	>400	-	14	20	-42.2				49	51.3	-4.69

	BCR-1[2]	AA	% Diff.	RGM-1[3]	AA	% Diff.				GSP-1[1]	ICP	% Diff.
J.												
Cu	18.4	18	2.2	11	12	-9.1				35	33	5.71

1. Abbey, 1978.
2. Flanagan, 1976.
3. Abbey, 1983.

A. ICP, U.S. Geological Survey (U.S.G.S.).
B. Inductively coupled plasma emission spectroscopy (ICP), Barringer-Magenta, Ltd., Toronto.
C. Titration, U.S.G.S.
D. Colorimetric, U.S.G.S.
E. INAA, U.S.G.S.
F. Instrumental Neutron Activation Analysis (INAA), Lawrence Livermore National Laboratory (LLNL).
G. ICP, U.S.G.S.
H. Graphite furnace atomic absorption, U.S.G.S.
I. ICP, Barringer-Magenta, Ltd., Toronto.
J. Flame atomic absorption, U.S.G.S.

CHEMICAL COMPOSITIONS OF THE ELKHORN MOUNTAINS VOLCANICS

Fifteen samples of lava flows and twenty-three samples from ash-flow sheets were analyzed (results are shown in Tables 2 and 3). The analyses of the lava flows in Table 2 are arranged in stratigraphic order and are numbered from 1 through 15, youngest to oldest. Table 3 contains analyses of welded tuff samples from the ash-flow sheets. Like those of the lava flows, these are arranged according to stratigraphic position. Analyses of welded tuffs are lettered from A through X (there is no B), with sample A being the youngest at the top of the stratigraphic column. The numbers and letters assigned to the lava flow samples and ash-flow sheet samples (Tables 2 and 3) are used in the following figures presenting chemical relationships where needed to indicate specific samples and also in Figure 4, which shows the relative positions of these samples in the stratigraphic sections previously described. All of the chemical analyses (Tables 2 and 3) were recalculated anhydrous and were normalized to 100% in order to compare the entire suite on the same basis.

The Elkhorn Mountains Volcanics-Boulder batholith association has been described as calc-alkaline (Tilling, 1973). However, of the samples from the study area, the older lava group (#10 through 15) and some of the ash-flow samples (A, C, O, P, Q, R, T) fall into the tholeiitic field of Miyashiro (1974) in Figure 5.

Figure 5 also shows that the new analyses do not represent any of the highly silicic volcanic rocks reported in previous studies (i.e., Knopf, 1957; Klepper and others, 1957; Ruppel, 1963; Smedes, 1966; Robinson and Marvin, 1967; Tilling, unpub. data). These silicic samples occur in welded tuffs of the middle member. There are at least two explanations for the lack of such samples in the new analyses. Highly silicic volcanic rocks may have been present in the unstudied,

Table 2. Chemical analyses of lava flows.

Stratigraphic Unit	Younger lava group VIII								V	Older lava group II					
Sample Number	1	2	3	4	5	6	7	8	9	10	11	12	13	14	15
Major Elements[1], weight %															
SiO_2	56.6	53.4	52.3	59.3	59.6	59.3	59.2	55.6	55.6	62.5	60.7	61.7	60.2	58.5	57.7
Al_2O_3	12.2	16.2	12.4	13.5	12.4	14.6	12.3	13.0	17.7	16.3	16.7	16.1	19.5	16.4	19.4
Fe_2O_3(T)	9.3	9.5	10.1	7.2	9.0	8.2	8.9	8.8	7.3	5.8	6.9	6.3	4.9	8.5	6.0
MgO	8.8	5.4	10.8	6.6	4.7	3.3	6.8	7.9	5.4	0.9	1.8	1.4	0.6	3.2	1.8
CaO	7.0	6.5	8.3	6.0	7.0	6.7	6.8	8.4	7.9	5.4	4.7	5.3	6.1	6.2	5.7
Na_2O	2.5	3.0	1.8	1.9	2.7	2.9	1.6	1.9	3.2	3.3	3.4	3.5	3.1	3.4	3.8
K_2O	2.7	4.3	3.0	4.4	3.4	3.6	2.6	3.3	1.7	4.2	4.2	4.1	4.0	2.3	4.0
TiO_2	.66	.93	.78	.76	.70	.82	.72	.69	.75	1.1	1.1	1.1	1.1	.92	1.1
P_2O_5	.34	.46	.41	.34	.35	.42	.35	3.6	.28	.49	.49	.47	.49	.43	.42
MnO	.17	.27	.15	.14	.16	.13	.12	.14	.15	.12	.12	.10	.08	.19	.09
Trace Elements, ppm															
Ba	691	1115	600	733	734	803	814	646	710	1414	844	1006	939	1243	1358
Co	38.3	33.0	43.7	31.0	29.6	32.8	35.2	37.0	31.6	12.3	12.6	13.2	16.9	10.9	15.3
Cr	510	246	586	414	422	246	443	452	323	2.3	2.2	4.9	17.9	17.9	21.3
Cs	2.0	.4	11.3	3.4	2.8	.3	2.1	6.8	1.3	2.5	5.9	1.4	.8	4.0	.6
Cu[1]	14.5	33.7	48.9	25.7	65.9	31.1	48.2	37.4	46.3	26.6	12.6	40.4	85.6	18.6	18.5
Hf	3.1	4.6	2.5	5.1	3.4	4.7	3.2	3.1	2.9	6.5	5.7	6.4	5.2	6.8	6.1
Ni[1]	152	54	166	143	81	47	94	108	74	9	9	9	13	11	17
Rb	57	100	90	104	47	72	52	114	41	106	139	114	49	95	105

Table 2 (continued).

Stratigraphic Unit	Younger lava group VIII								V	Older lava group II					
Sample Number	1	2	3	4	5	6	7	8	9	10	11	12	13	14	15
Trace Elements, ppm (continued)															
Sb	n.d.	.5	n.d.	.5	1.8	.1	n.d.	.4	n.d.	.2	.2	.5	.2	1.5	.2
Sc	25.4	22.4	26.3	17.9	26.5	20.6	26.1	25.9	20.0	12.2	12.6	12.8	17.9	10.9	12.3
Sr[1]	640	955	662	450	650	943	712	712	948	795	876	799	953	1070	926
Ta	.3	.5	.2	.6	.3	.5	.3	.2	.4	.9	.9	.9	.6	.9	.8
Th	3.9	6.6	3.5	7.8	4.5	6.8	4.3	4.6	4.0	11.5	10.3	11.1	6.9	10.4	9.5
U	.6	1.4	n.d.	1.9	.7	1.1	n.d.	.6	1.1	3.1	n.d.	2.4	5.9	2.6	2.0
V[1]	137	131	157	118	157	144	141	137	159	133	142	144	121	142	114
Zn	95	148	92	106	91	128	86	97	91	97	110	109	120	59	104
Zr[1]	89	153	89	152	86	140	92	97	85	207	185	193	185	149	163
La	20	21	33	36	21	30	21	22	21	48	46	48	43	48	47
Ce	38	38	62	67	44	58	43	43	38	91	82	88	79	93	87
Sm	3.7	3.7	5.0	5.2	3.8	4.5	4.1	3.7	3.2	6.5	6.4	6.4	5.3	6.9	6.7
Eu	1.08	.99	1.37	1.37	1.13	1.34	1.15	1.12	1.11	1.84	1.62	1.78	1.83	1.88	1.85
Tb	.46	.44	.57	.58	.49	.58	.50	.49	.39	.71	.72	.75	.69	.76	.72
Yb	1.9	1.3	2.0	2.4	1.7	2.1	2.0	1.8	1.7	2.6	2.1	2.8	2.9	3.1	2.6
Lu	.31	.30	.42	.45	.24	.37	.29	.19	.30	.48	.62	.47	.34	.50	.49

Analyses normalized to 100% anhydrous.
1 = ICP, Barringer Magenta, Ltd., Toronto.
All others by INAA, Lawrence Livermore National Laboratory.

Table 3. Chemical analyses of ash-flow sheets.

Stratigraphic Unit	XIII	XII					XI			X	IX	
Sample Number	A	C	D	E	F	G	H	I	J	K	L	M
Major Elements[1], weight %												
SiO_2	68.5	66.9	63.6	64.8	64.5	65.7	66.9	66.7	66.6	67.4	64.1	68.7
Al_2O_3	16.8	18.4	17.6	17.7	17.9	16.7	17.8	17.3	17.2	16.3	17.2	16.5
Fe_2O_3	1.8	1.3	2.4	2.1	2.7	2.3	2.1	1.9	1.9	1.6	2.8	3.0
FeO	1.4	2.6	1.8	2.0	1.4	1.1	1.4	1.2	1.0	1.6	1.7	.4
MgO	.7	1.0	1.5	1.6	1.3	2.5	1.2	1.1	1.1	1.3	1.6	.5
CaO	1.4	2.0	4.6	3.6	4.5	2.6	1.6	1.7	2.7	4.6	4.1	1.2
Na_2O	4.1	3.2	3.6	2.9	2.6	2.6	4.1	4.5	4.0	1.7	2.9	3.2
K_2O	4.4	3.4	3.8	4.3	3.9	5.4	4.0	4.6	4.5	4.3	4.3	5.6
TiO_2	.74	.78	.75	.80	.83	.84	.80	.66	.62	.75	.77	.79
P_2O_5	.09	.22	.10	.25	.23	.20	.16	.19	.20	.21	.31	.11
MnO	.14	.09	.13	.09	.13	.07	.07	.07	.08	.10	.11	.06
Trace Elements, ppm												
Ba	1490	1370	1780	1570	1600	1370	1400	1430	1400	1760	1270	1460
Co	2.9	5.6	6.0	6.0	5.6	4.9	5.5	5.0	4.6	4.9	7.2	2.8
Cr	5.0	15.9*	15.4*	6.3	13.6*	7.6	36.9*	5.5	5.7	5.5	19.1*	6.3
Cs	2.9	2.1	2.5	1.6	2.6	3.4	5.2	2.9	1.2	2.5	3.1	2.5
Cu	14	n.d.	10	13	18	12	10	13	n.d.	10	46	21
Hf	7.8	5.3	5.6	5.5	5.2	6.2	6.2	6.3	6.4	5.8	5.6	7.7
Ni	n.d.	8	57	n.d.	6	8	5	n.d.	n.d.	4	9	6
Rb	140	106	106	110	108	149	113	118	123	136	125	159
Sb	1.0	.4	.3	.5	.5	.5	.3	.4	.3	.4	.5	.6
Sc	8.4	10.6	11.1	11.2	10.3	10.1	9.0	8.7	8.9	10.4	10.5	8.7
Sr	400	600	1000	77	1200	490	430	460	470	680	630	360
Ta	1.3	.9	.9	.9	.8	1.0	1.0	1.0	1.0	1.0	.9	1.3
Th	16.4	11.1	11.3	11.3	10.9	12.5	11.4	11.7	12.1	11.8	11.5	16.3
U	3.9	2.6	3.8	2.6	2.8	3.0	2.7	2.8	2.9	2.8	2.8	3.6
V	28	66	85	100	75	58	62	70	55	76	74	41
Y	25	23	24	23	23	25	22	21	21	24	23	23
Zn	40	74	79	79	70	71	63	57	58	75	77	51
Zr	310	240	270	240	250	340	270	240	280	250	240	290
La	56.8	47.2	49.6	47.9	47.2	47.8	47.5	49.0	47.9	49.5	49.3	52.5
Ce	104	84	88	85	85	89	85	84	84	89	87	93
Sm	7.9	6.9	7.3	6.9	6.8	7.3	6.4	6.7	6.6	7.2	7.1	6.8
Eu	1.57	1.72	1.82	1.72	1.75	1.64	1.57	1.55	1.50	1.73	1.69	1.54
Tb	.83	.70	.76	.86	.68	.72	.69	.80	.80	.71	.69	.69
Yb	2.8	2.3	2.5	2.7	2.3	2.6	2.3	2.7	2.5	2.6	2.5	2.3
Lu	.44	.37	.38	.38	.35	.41	.35	.39	.39	.39	.37	.38

32

Table 3 (continued).

Stratigraphic Unit	VII					VI	IV	III			I
Sample Number	N	O	P	Q	R	S	T	U	V	W	X

Major Elements[1], weight %

	N	O	P	Q	R	S	T	U	V	W	X
SiO_2	64.1	63.7	58.6	61.6	61.3	67.5	60.1	63.8	64.4	66.6	64.8
Al_2O_3	17.1	17.2	18.4	17.2	17.3	15.9	17.4	16.8	17.2	18.2	17.0
Fe_2O_3	4.3	4.5	3.8	3.5	3.7	2.6	2.2	2.4	2.2	1.4	.80
FeO	2.6	1.4	3.1	2.8	2.3	1.6	5.5	4.2	3.1	3.5	3.7
MgO	3.1	1.4	2.2	2.1	1.8	1.4	2.4	2.1	1.6	1.9	1.5
CaO	2.6	2.1	4.0	4.8	3.5	3.5	5.6	3.9	5.3	2.0	4.0
Na_2O	1.9	1.2	2.0.	2.2	1.3	1.4	2.4	1.6	1.4	1.8	1.8
K_2O	2.9	7.2	6.3	4.5	7.5	4.8	2.7	3.8	3.5	3.4	4.4
TiO_2	.82	.82	.89	.81	.80	.89	.96	.83	.90	.82	1.4
P_2O_5	.42	.36	.44	.38	.35	.31	.45	.38	.39	.36	.50
MnO	.21	.10	.21	.15	.12	.07	.17	.09	.12	.11	.15

Trace Elements[2], ppm

	N	O	P	Q	R	S	T	U	V	W	X
Ba	948	1830	1130	1250	1710	1740	768	901	1180	936	1560
Co	13.8	11.4	15.1	13.8	11.1	6.5	15.3	9.7	8.3	7.9	9.8
Cr	48.3*	47.6*	30.0*	36.4*	39.9*	9.3	26.3*	12.1	9.5	10.2	18.1*
Cs	2.2	2.1	1.3	1.1	1.9	1.8	33.3	11.5	7.6	8.6	6.6
Cu	24	37	33	40	35	32	49	24	18	13	16
Hf	3.9	4.1	4.3	4.1	3.8	6.4	4.0	5.8	5.8	5.8	8.4
Ni	47	41	33	30	30	17	17	8	9	6	14
Rb	85	164	134	106	130	111	111	126	109	104	164
Sb	.3	.3	1.3	.3	.3	.2	1.2	n.d.	.4	.2	.4
Sc	12.5	11.8	12.6	12.6	11.1	10.6	17.6	13.7	12.9	12.3	12.1
Sr	470	490	700	680	590	720	800	610	750	610	650
Ta	.6	.6	.6	.6	.5	1.1	.6	.9	1.0	1.0	2.1
Th	5.9	6.2	6.6	6.0	6.0	12.2	6.6	9.6	9.8	10.1	19.8
U	1.5	1.7	1.7	1.6	1.7	2.7	1.4	1.7	2.1	1.9	4.4
V	140	160	190	160	140	120	220	110	100	110	180
Y	20	20	21	18	16	21	20	25	25	25	24
Zn	82	76	96	87	73	63	99	83	84	88	47
Zr	180	190	310	350	180	360	210	260	240	260	410
La	29.3	31.0.	30.8	29.1	30.5	44.6	32.3	45.7	44.5	46.2	73.1
Ce	53	55	57	54	54	82	59	80	80	83	126
Sm	5.0	5.2	5.3	5.1	5.0	6.7	6.1	7.5	7.1	7.4	8.5
Eu	1.32	1.29	1.40	1.33	1.28	1.41	1.50	1.80	1.72	1.67	1.62
Tb	.57	.54	.62	.60	.61	.83	.68	.82	.84	.82	.80
Yb	1.9	1.9	2.1	2.0	2.0	2.5	2.2	2.6	2.5	2.6	2.8
Lu	.32	.30	.35	.31	.30	.35	.36	.41	.41	.40	.39

Analyses normalized to 100% anhydrous.
1 = All major elements by ICP, except FeO by titration, and TiO_2 and P_2O_5 colorimetrically (U.S. Geological Survey, J. Gillison, Analyst).
2 = All trace elements by INAA (U.S. Geological Survey, G. A. Wandless, Analyst), except Cu by flame atomic absorption, Ni and V by graphite furnace atomic absorption, and Sr, Y, and Zr by ICP (U.S. Geological Survey, W. D'Angelo, Analyst).
*Cr analyses suspected of contamination.
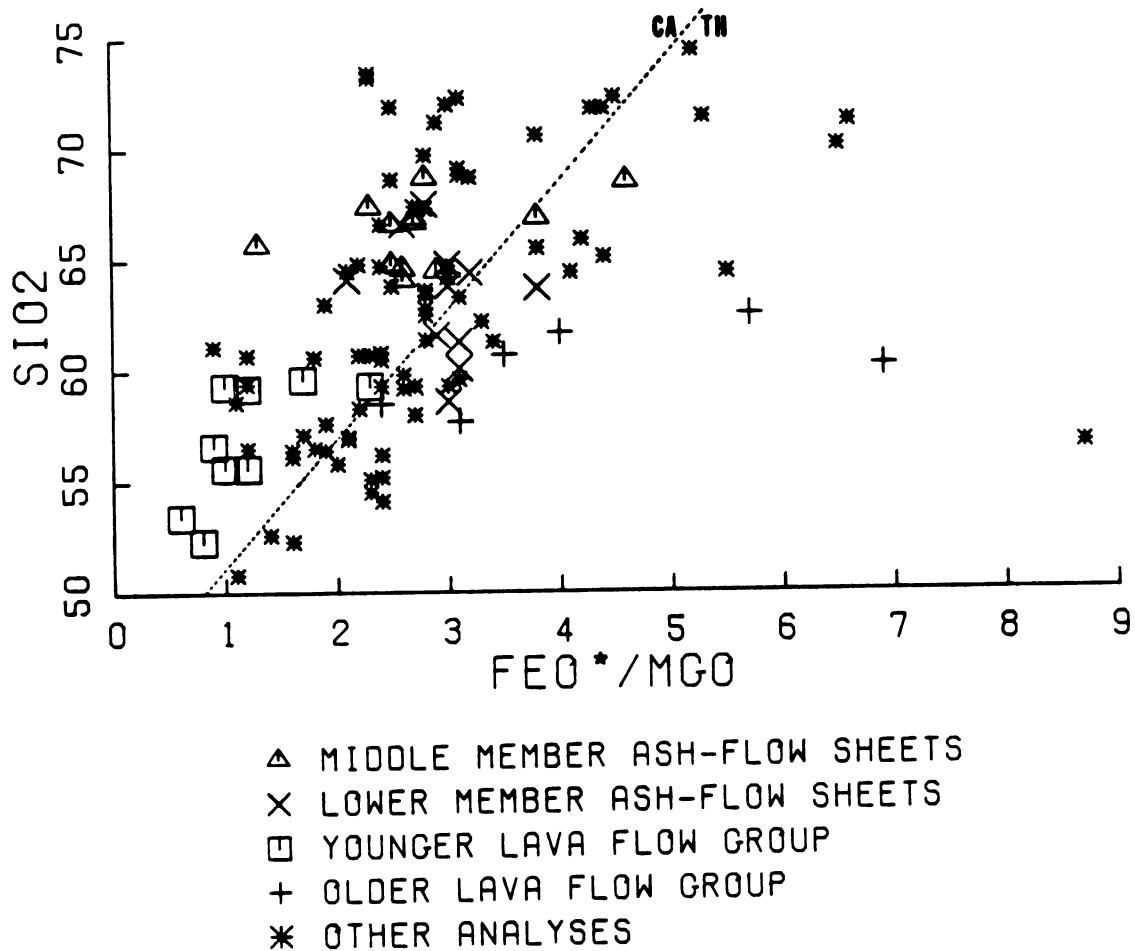
33

Figure 5. Plot of SiO_2 against FeO*/MgO of all available Elkhorn Mountains Volcanics analyses. Data from Tables 2 and 3, Mutschler and others (1976a and b), and Tilling (unpub. data). CA = calc-alkaline, TH = tholeiitic.

altered upper part of the middle member or in the covered region to the north of the study area (Figure 3). This possibly implies that the ash flows in the middle member became more silicic with time. An alternate explanation is that the highly silicic volcanic rocks are present in the study area, in either the non-or partly welded portions of the ash-flow sheets or in poorly exposed parts of the stratigraphic section, that is, in the unsampled portions of the volcanic section. In this case, the silica variability might be entirely within ash-flow sheets.

Major Elements

Lava Flows. The chemical analyses of the lava flows fall into two groups (Table 2) and it is convenient to refer to these groups as the younger lava flow group (VIII and V) and the older lava flow group (II) in the following discussion.

The two groups of lava flows in the lower member differ from one another in both major and trace element abundances (Table 2). The younger group (#1-9) is distinctly less evolved in terms of SiO_2 content in comparison to the older group (#10-15).

The major element variation diagrams of the lavas (Figure 6) illustrate the following characteristics of the two lava flow groups:

1) The SiO_2 contents of the younger lava flow group are generally lower than those of the older group. Silica ranges from 52.3 to 59.6 weight % in the younger group and from 57.7 to 62.5 weight % in the older group.

2) The Al_2O_3, Na_2O, TiO_2, and, to some degree, P_2O_5 contents of the younger group are generally lower than in the older group. However, the overall ranges in TiO_2 and P_2O_5 are very small, indicating no statistically significant difference in the abundances of these oxides.

3) The CaO, FeO, and MgO abundances of the younger lava flow group are generally higher than those of the older group, consistent with the lower SiO_2 contents in the younger lavas and with their less evolved character.
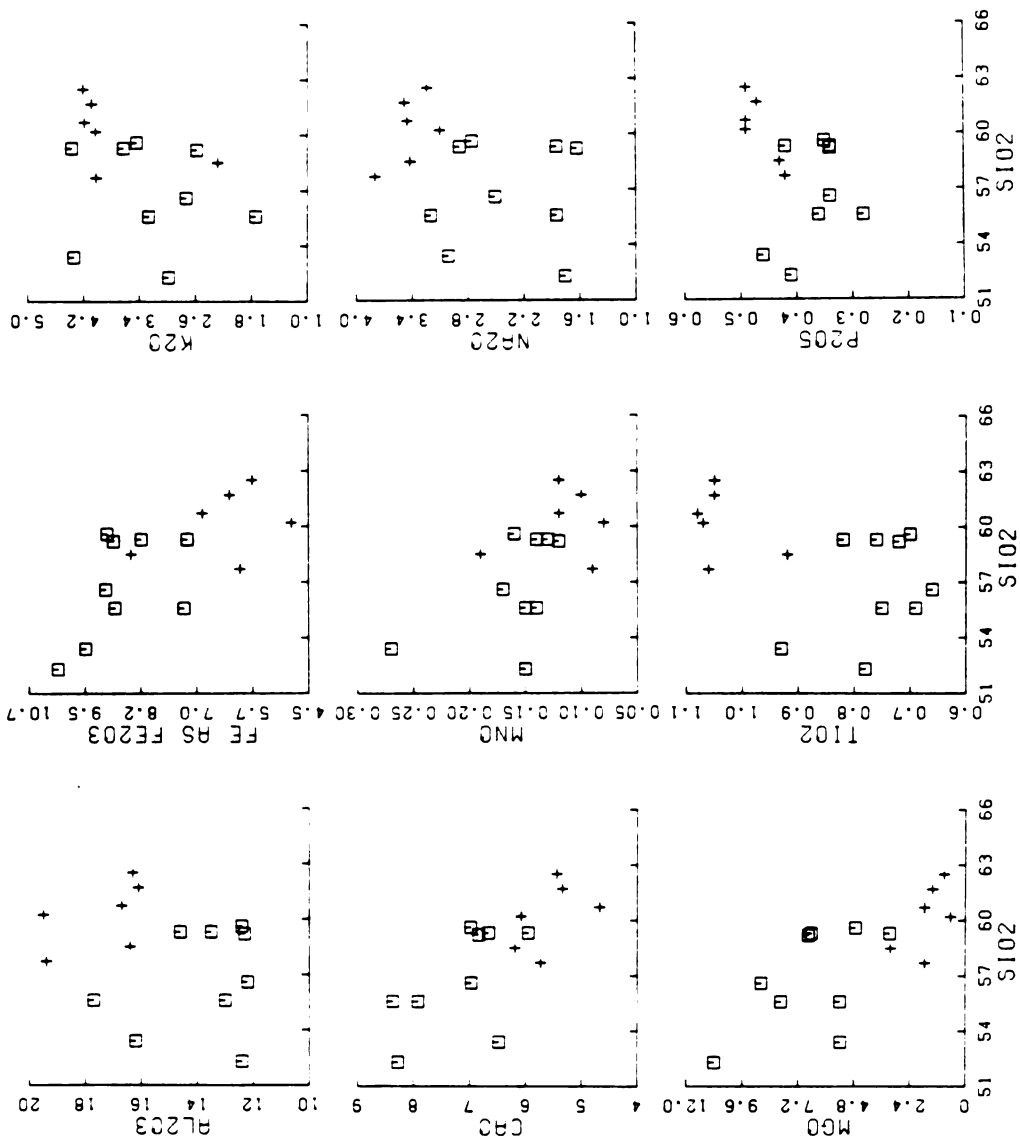
Figure 6. Major-element variation diagrams of the lava flows. Data of Table 2. Symbols as in Figure 5.

4) The K_2O, Na_2O, and CaO abundances in the younger lavas are highly variable. The older lavas are uniformly high in K_2O (about 4.0%), with the exception of sample 14, and in Na_2O (about 3.4%), and are low in CaO (see Figure 7).

The variable distribution of K_2O, Na_2O, and CaO within the younger lava flow group could indicate mobility of these elements. Element mobility in volcanic rocks has been documented previously (Lipman, 1965; Noble, 1967). There is no consistent enrichment of K_2O with loss of Na_2O, as would be expected from other studies (Lipman, 1965; Noble, 1967), nor is the variability of CaO in the leached samples any different from that in the non-leached samples. In the Elkhorn Mountains Volcanics, mobility was probably due to the combined post-depositional alteration processes of de-vitrification, hydration, contact metamorphism and others. Systematic linear trends of the other oxides plotted against SiO_2 are interpreted as indicating that they have been relatively immobile.

Ash-flow Tuffs. Variation diagrams of the major element oxides in the ash-flow sheets (Figure 7) can be used to illustrate several differences between ash-flow sheets from the lower member (analyses N through X) and those of the middle member (analyses A and C through M).

1) In general, the highest SiO_2 and Na_2O contents are found in the middle member. Variability in Na_2O may be due to Na_2 mobility.

2) Al_2O_3, MgO, CaO, K_2O, and MnO ranges are similar in all the ash-flow sheet samples, although the distributions of Al_2O_3, MgO, and MnO are considerably restricted in comparison to those of CaO and K_2O. The possibility of mobility must be kept in mind when assessing the K_2O and CaO variability.

3) FeO and P_2O_5 are both generally less abundant in the middle member, with some exceptions. Although the ranges of FeO and Fe_2O_3 concentrations of

37
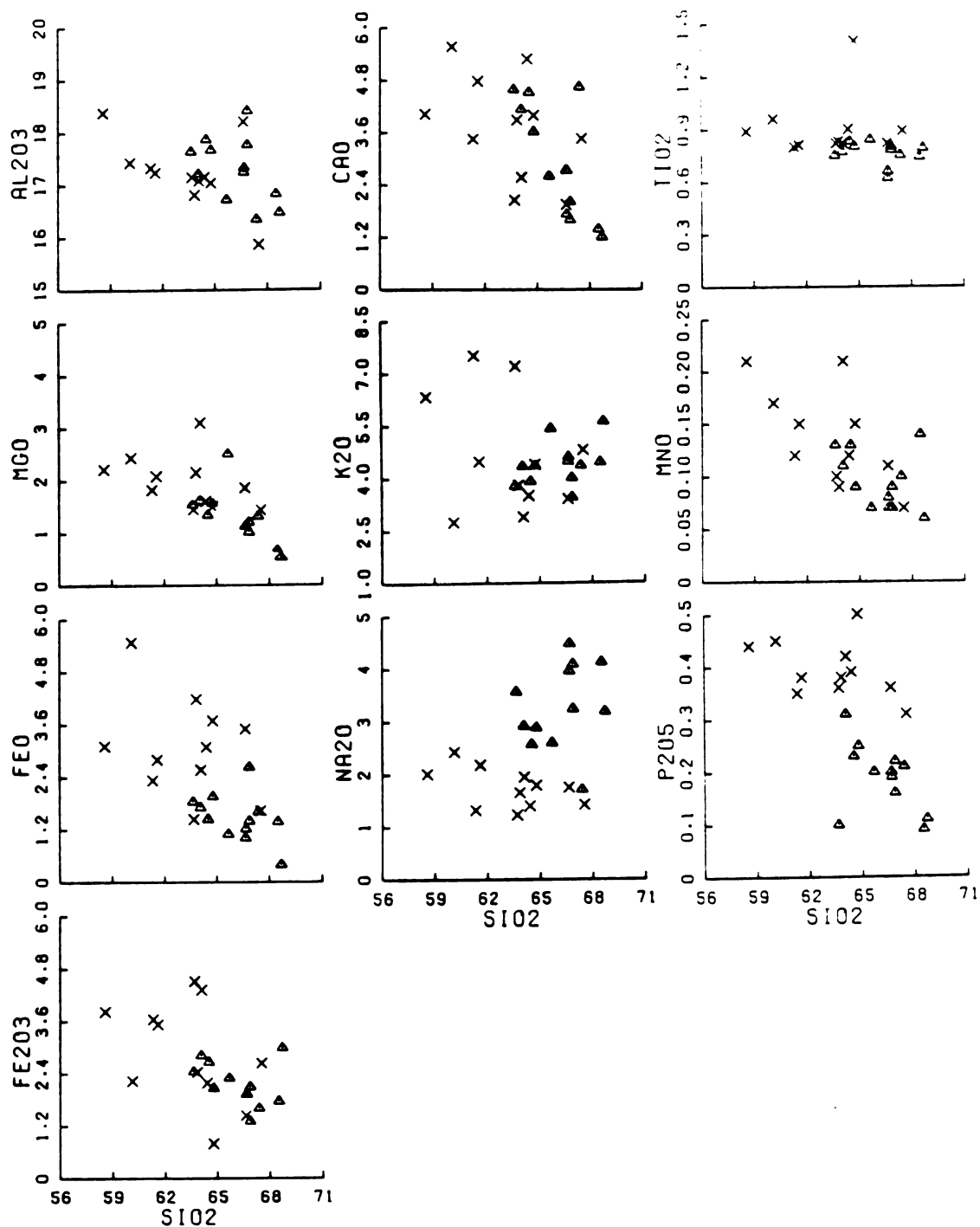
Figure 7. Major-element variation diagrams of the ash-flow sheets. Data of Table 3. Symbols as in Figure 5.

the two members overlap, the variability of FeO and Fe_2O_3 in the middle member is less than in the lower member.

Trace Elements

The samples were analysed for Ba, Co, Cr, Cs, Cu, Hf, Ni, Rb, Sb, Sc, Sr, Ta, Th, U, V (not measured in the lava flows), Zn, Zr, and the rare earth elements (Tables 2 and 3). Some important differences in the abundances of some of the trace elements can be noted, especially when these elements are plotted against thorium (Figure 8). Thorium was used as reference because 1) it does not appear to be mobile during crystallization and alteration of silicic lavas and ash flows (Rosholt and Noble, 1969; Rosholt and others, 1971), 2) analytical precision is good, and 3) it is present over a range of concentrations. Because thorium is an incompatible element during differentiation processes, it also is an excellent indicator of the degree of chemical evolution of a suite of cogenetic igneous rocks.

Except for sample 13 (indicated on Ni plot), the older lava group contains Th greater than 8 ppm, in comparison to the younger group less than 8 ppm. Chromium, Co, Ni, and Sc are strongly bimodal in distribution between the two major lava groups (Figure 8). Furthermore, in the younger lava group these elements show sharply negative slopes against Th. As will be discussed below, such a trend in plots of compatible elements against an incompatible element is consistent with a history dominated by processes of crystal-liquid equilibrium, either partial melting or fractional crystallization.

Except for samples X and S (indicated on Ni and Ta plots), the lower member ash-flow sheets contain less Th than those in the middle member (Figure 8). Sample S is similar to the middle member ash-flow sheet samples in Th content, and sample X is the most Th rich in the entire sequence. All but two
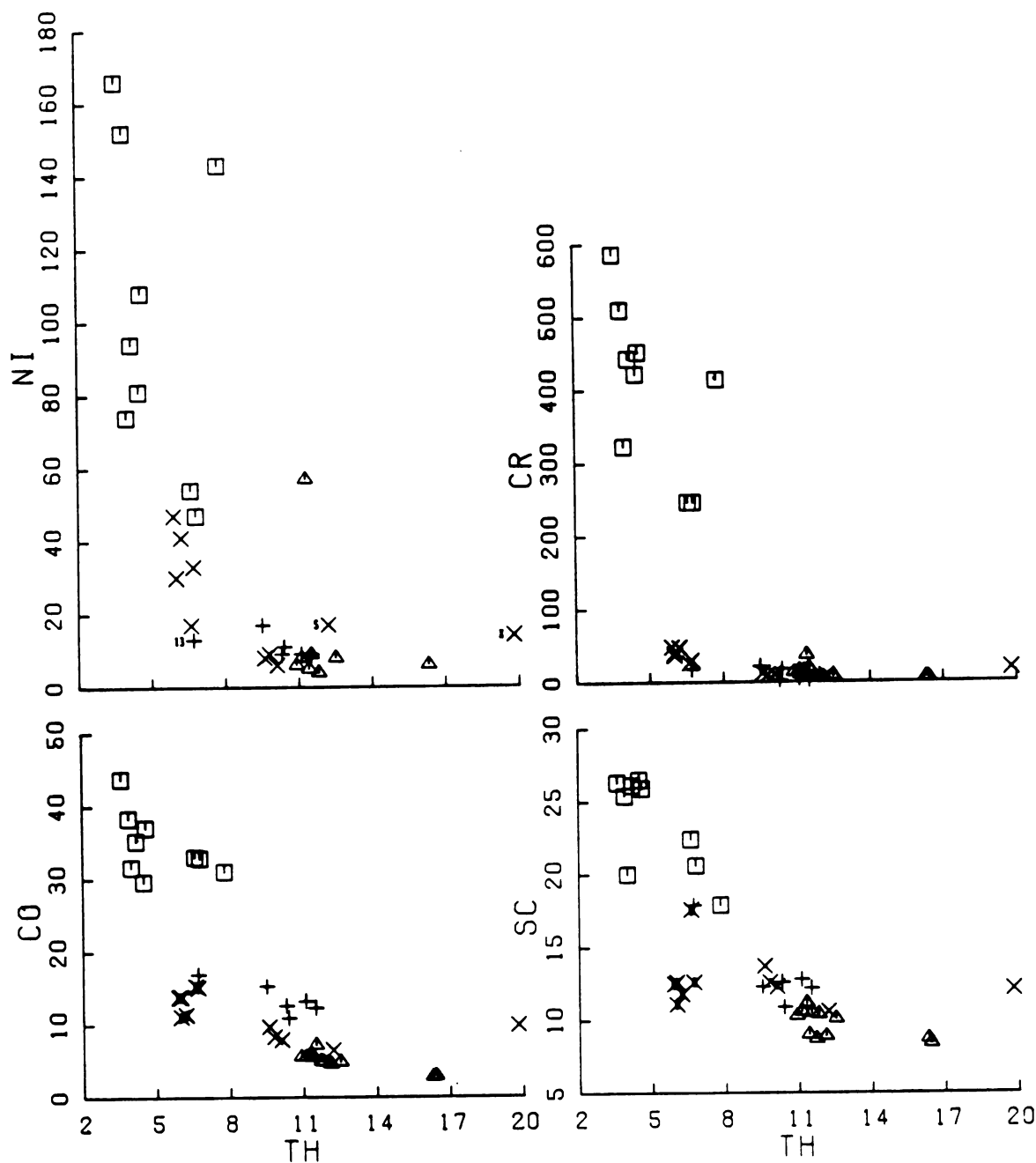
Figure 8. Plots of Ba, Ce, Co, Cr, Cs, Hf, Ni, Rb, Sc, Sr, Ta, and Zr against Th. Trace element data of Tables 2 and 3. Roman numerals, Arabic numbers, and letters correspond to sample groups and analyses of Tables 2 and 3 and Figure 4. In plots of Co and Sc, symbol ✖ indicates ash-flow sheets IV and VII. In plots of Rb, Ba, Sr, and Cs, a solid box indicates lava unit V, solid triangles indicate ash-flow sheet XII, and dashed outlines indicate ash-flow sheets III and VII.
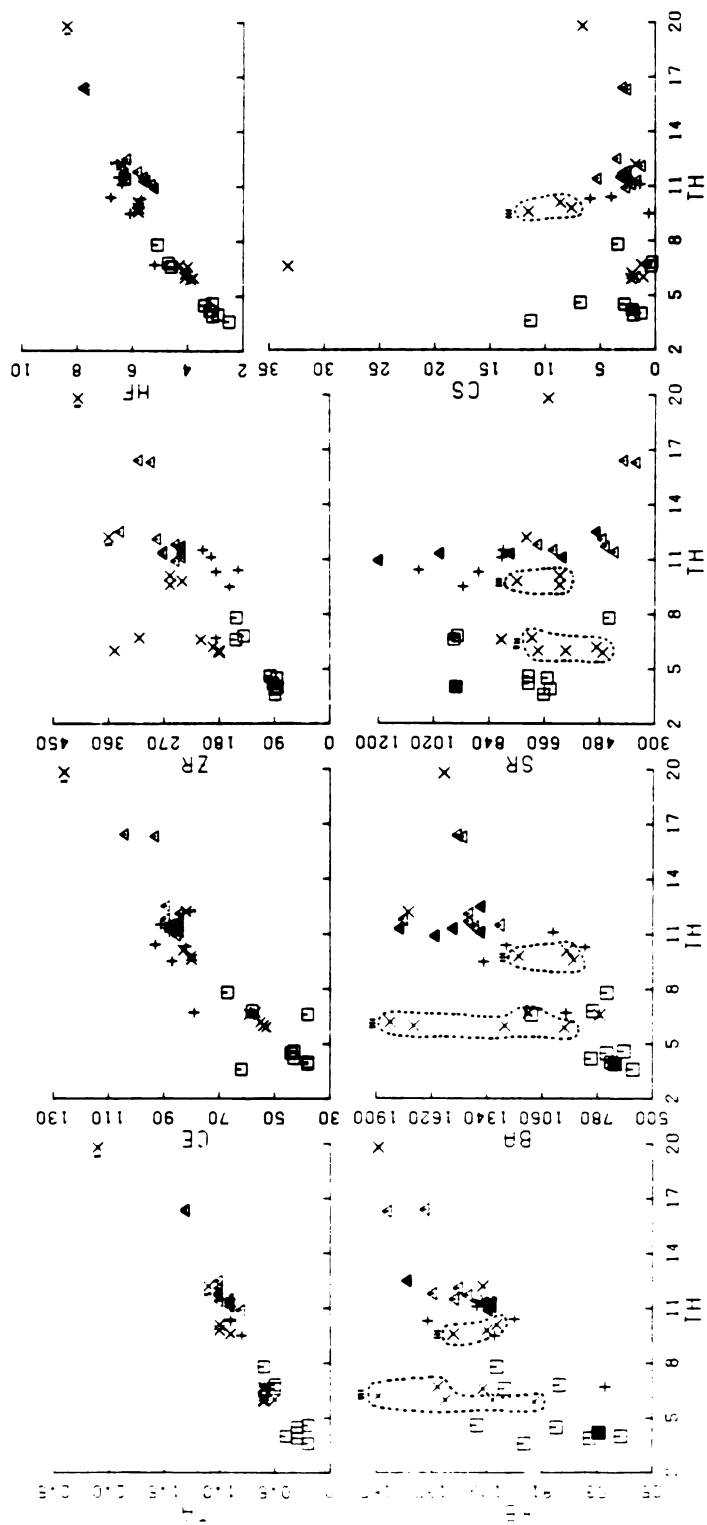
Figure 8 (continued).

samples from the middle member cluster between 10.5 and 12.5 ppm Th; the exceptions are samples A and M, containing 16.4 and 16.3 ppm Th, respectively.

Plots of the compatible elements Sc and Co, against Th show that samples N, O, P, Q, R (unit VII), and possibly T (unit IV) fall on a generally separate trend from the other samples of ash-flow sheets (Figure 8). Most of the remaining samples from ash-flow sheets show decreasing abundances of these elements with increasing Th. Sample X, however, is consistently off of either possible trend. The plots of Ce, Hf, Ta, and, to a lesser degree, Zr (Figure 8) show good linear variation with Th in all of the samples. In lower member sample S, the concentrations for all four of these imcompatible elements are similar to those of the ash-flow sheets in the middle member. The concentrations of Ce, Hf, Ta, and Zr increase with Th and with time, except in sample X, from the base of the stratigraphic sequence, which consistently shows the most evolved character of all the ash-flow sheet samples.

The possible mobility of K_2O, Na_2O, and CaO resulting from post-eruption alteration, seen in the scatter of points in Figures 6 and 7, may also be accompanied by mobility of related trace elements as well. All three major elements are plotted against Th in Figure 9. Evidence for mobility is indicated by wide ranges of these elements in lava group VIII, especially of K_2O, and in ash-flow sheet VIII (Figure 9). Rubidium may have been mobile in ash-flow sheets III, VII, and at least sample G of sheet XII, and in lava group VIII (Figure 8). Barium has apparently been mobile in ash-flow sheets III, VII, and XII (Figure 8). Strontium may have been mobile in sheets III, VII, and XII (Figure 8). Cesium mobility is indicated in lava group VIII and II, ash-flow sheet III and IV, and possibly throughout the entire middle member (Figure 8). It is important to distinguish the scatter within individual units, best explained by mobility of·the particular elements during post-eruption alteration, from the overall positive

Figure 9. Plots of K_2O, Na_2O, and CaO against Th. Data of Tables 2 and 3. Solid boxes indicate lava group VIII. Ash-flow sheet VII indicated by ✖ . Other symbols as in Figure 5.
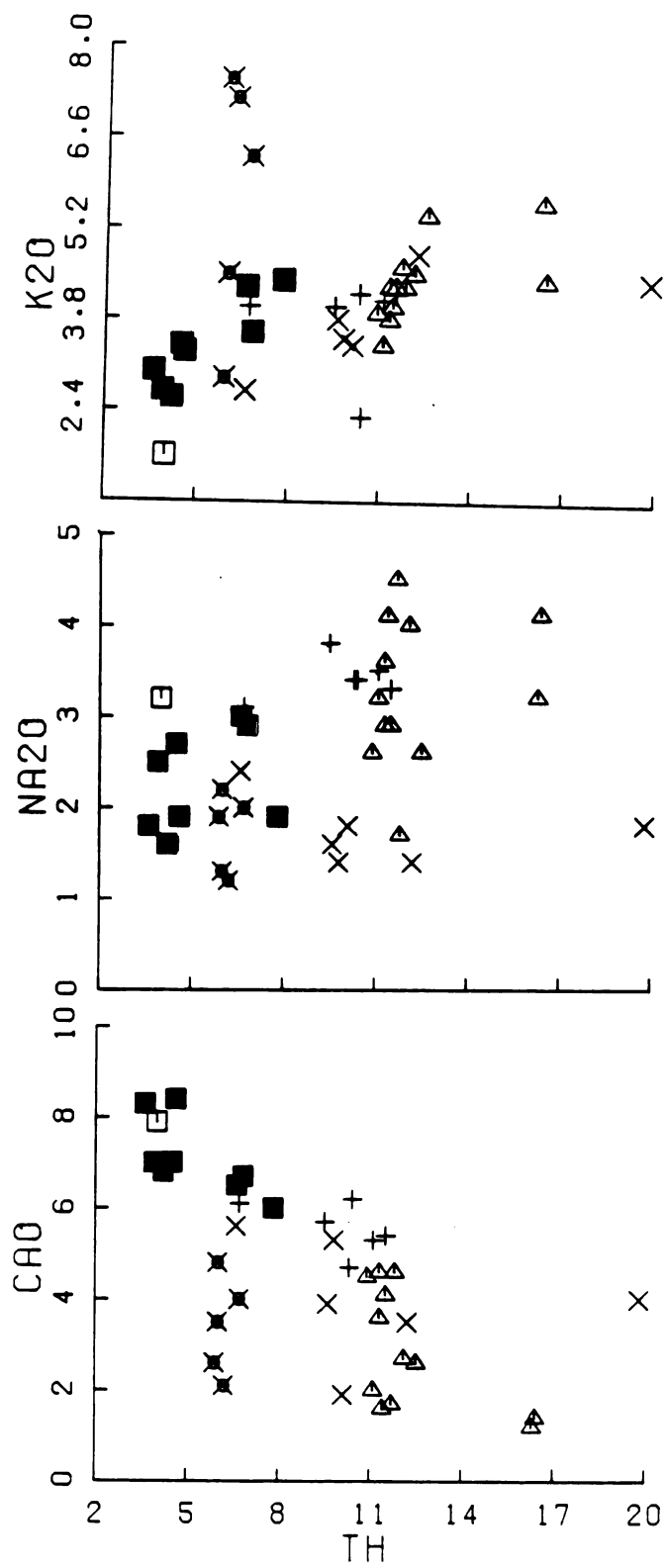
Figure 9.

correlation of Rb and Ba with Th. This positive trend may be taken as a suggestion of the original variation of Rb and Ba with Th.

Chondrite-normalized rare earth element (REE) profiles (Figure 10) for the lava flows, lower member ash-flow sheet samples, and middle member ash-flow sheet samples have common aspects. None shows a distinct europium anomaly. The older lava group contains slightly greater REE abundances than the younger group, which is consistent with the more evolved character of these lavas. The REE profiles in the middle member are extremely uniform (Figure 10).

Ash-fall Analyses

Although there are different kinds of ash falls, some are directly associated with the eruption and emplacement of ash-flow sheets, and thus may be products of the same processes which produced the ash-flow sheets. Because compositional zoning in ash flow sheets is commonly assumed to reflect pre-eruption zonation in the magma body (Smith and Bailey, 1966; Lipman and others, 1966; Smith, 1979; Hildreth, 1981), and because ash falls plainly erupt before ash-flow sheets, an ash fall might sample the upper highest, most-evolved portions of the magmatic system. Chemical analyses of ash-fall units (Appendix) immediately below ash-flow sheets (Figure 4) were obtained in order to examine the possibility of one or more such ash falls showing the same chemical trends as the overlying ash-flow sheets, and hence might be co-genetic with that ash-flow. Preliminary inspection of the data from these rocks permitted no generalizations regarding any genetic relationship between the ash falls and the ash-flow sheets, and the ash fall analyses were omitted from the discussion of the geochemistry of the Elkhorn Mountains volcanics.

The absence of any observable relationship between logical ash fall - ash-flow sheet pairs may have several implications. If ash falls do sometimes sample the uppermost levels of the magma chamber, then perhaps the top parts of the

Figure 10. Chondrite-normalized rare earth element profiles for the Elkhorn Mountains Volcanics. (Data of Tables 1 and 2 normalized by values in Haskin and others, 1968). A. Lava flows. B. Lower Member ash-flow sheets. C. Middle Member ash-flow sheets. Symbols as in Figure 5.

Figure 10.

47
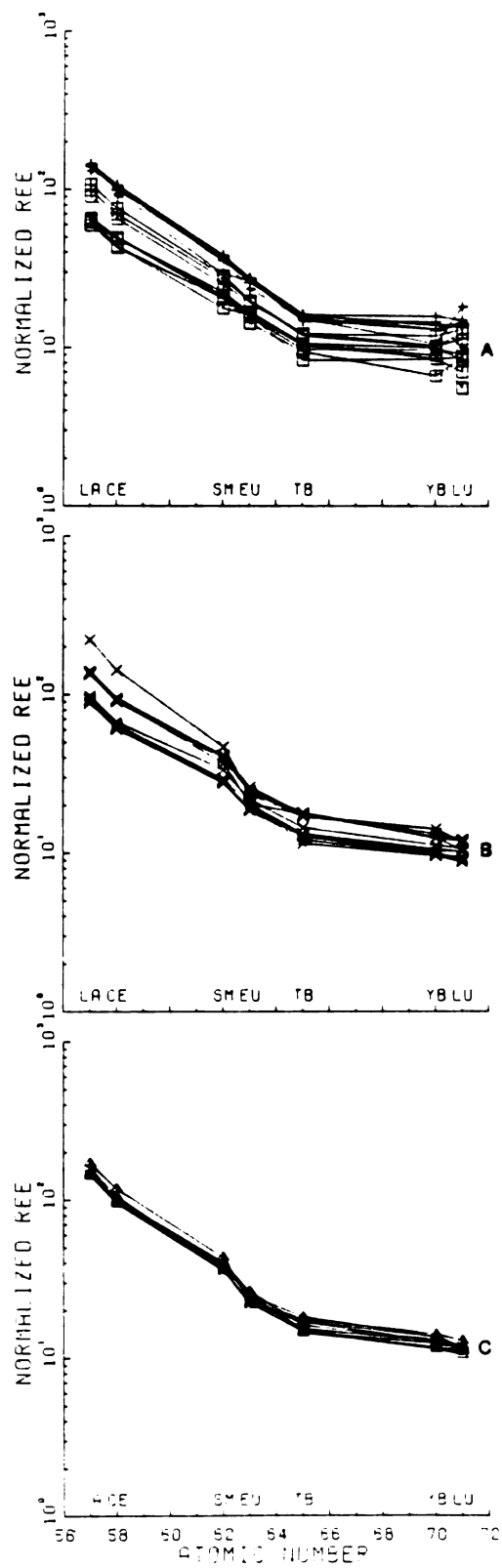
chambers are heterogeneous and not uniformly consistent with gradients present in the rest of the magma body. Alternatively, any evolutionary processes which might have been identified may not have been preserved in the ash-fall samples, which would be most susceptible to alteration processes. Conversely, ash falls may not sample just the uppermost levels of the magma chamber.

DISCUSSION

Interpretation of the chemical variation in the Elkhorn Mountains Volcanics may be made in terms of: 1) the chemical trends in the volcanic sequence, 2) the evidence of processes affecting the distinct groups of lava flows and ash-flow sheets, 3) the possible relationships between the lava flows and ash-flow sheets, and 4) the evolution of the entire system within the time frame represented in the study area. Finally, analysis of the geochemistry of the Elkhorn Mountains Volcanics and the Boulder batholith may be made in order to compare the different processes that influenced the volcanic and plutonic rocks.

Chemical Trends within the Volcanic Sequence - A Single Magmatic System

The chemical trends within the entire Elkhorn Mountains Volcanics sequence are consistent with the assumption that this sequence is related to the evolution of a single magmatic system, although not necessarily of a single magma chamber. The enrichment of the incompatible elements Ce, Ta, Hf, Zr, and Th (Figure 8) and of Ce and Yb (Figure 11) shows the positive, nearly linear trends of this sequence of volcanic rocks that range in SiO_2 from about 53% to 69%. However, the possibility of evolution in a single chamber is virtually precluded by trends in different groups of lava flows and ash-flow sheets (discussed below), that are interpreted as indicating that certain processes influenced the evolution of some groups but not of all. Instead, the magmatic system envisioned here would have consisted of several separately evolving bodies of magma which together reached batholitic dimensions, different portions and culminations of which were tapped to produce the lava flows and ash-flow sheets of the Elkhorn Mountains Volcanics.

49

Figure 11. Plot of Ce against Yb. Units indicated by Roman numerals. Symbols as in Figure 5.

Figure 11.

51
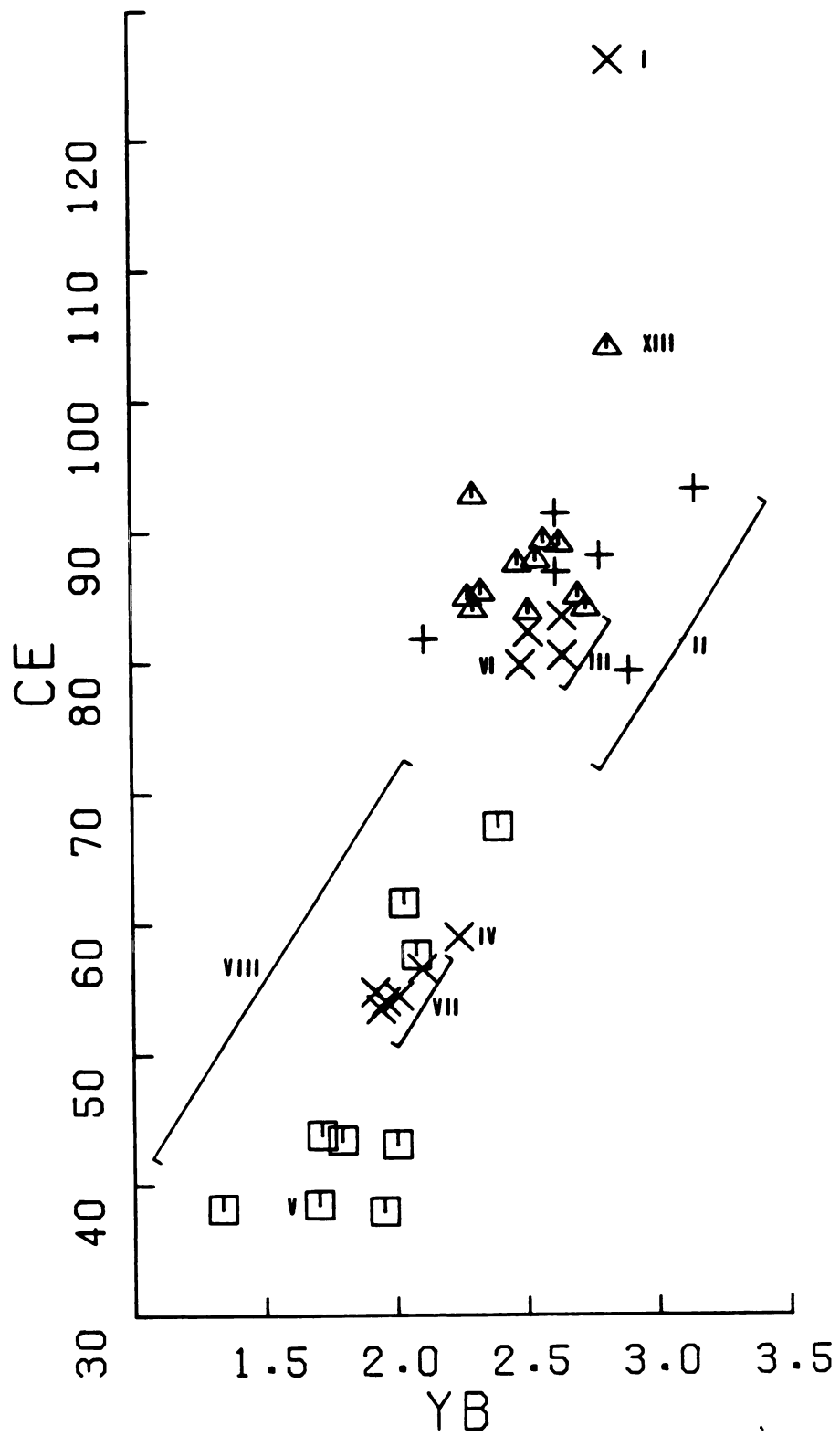
A plot of Ta against Th for the Elkhorn Mountains Volcanics compared with some other zoned systems permits further characterization of this proposed magmatic system (Figure 12). A noteworthy feature of this comparison is that the ranges of both Ta (from 0.2 to 2.1 ppm) and Th (from 3.5 to 19.8 ppm) in the entire suite of Elkhorn Mountains Volcanics, which consists of many lava flows and ash-flow sheets, are comparable to those of individual ash-flow sheets, such as LCT and HRT ((Lava Creek ash-flow tuff and Huckleberry Ridge ash-flow tuff, Yellowstone (Hildreth, 1981)). The relative constancy of the Th/Ta ratio, despite the many eruptive products, separated in time, provides compelling evidence that the entire Elkhorn Mountains Volcanics pile was derived from the same, single system.

Within the single dynamic system, however, different mechanisms of evolution produced chemical trends in the two lava groups and the ash-flow sheets preserved in the study area. The roles of some specific processes can be identified and others can be rejected on the basis of chemical evidence in the samples.

Evidence of Processes Affecting the Distinct Groups of Lava Flows and Ash-flow Sheets

The Ash-flow Sheets. The presence of a variety of lithologies in the lower member permits recognition of parts of five ash-flow sheets, based on significant changes in the stratigraphic sequence, as reflected in the alternations between bedded tuffs, lava flows, and volcanoclastic units. Using the same criteria, cooling breaks in the thick sequence of ash-flow sheets in the middle member can be placed below the lithologies from which samples K, J, G, and A were taken (Figure 4). Therefore, at least five ash-flow sheets can be distinguished in the middle member in the study area. This conclusion is reasonably consistent with 1) Smedes's statement that at least seven ash-flow sheets can be found in

52
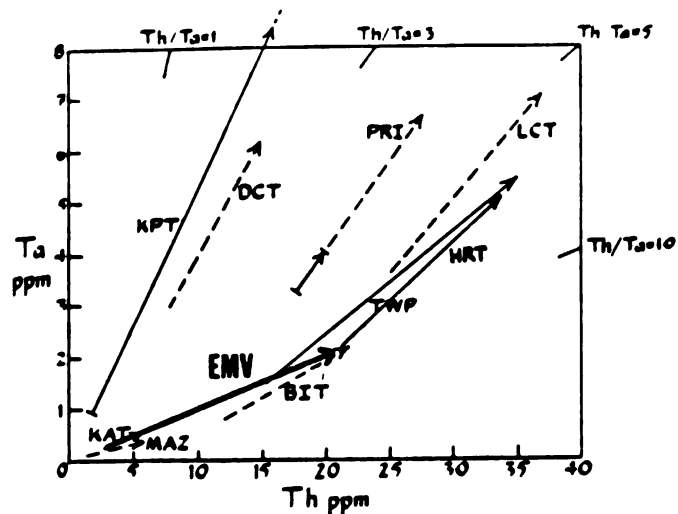
Figure 12. Plot of Ta against Th for the Elkhorn Mountains Volcanics compared with some other eruptive units. Data from Tables 1 and 2, Baker and McBirney (1985), and Hildreth (1981). Modified from Baker and McBirney (1985). EMV: Elkhorn Mountains Volcanics, southwestern Montana (Tables 1 and 2). KAT: Pumice-flow and Novarupta dome, Valley of Ten Thousand Smokes, Alaska. MAZ: Mazama (Pinnacles) pumice flow, Crater Lake, Oregon. TWP: Twin Peaks basalt-rhyolite complex, Utah. DCT: Devine Canyon tuff, Oregon. PRI: Sierra la Primavera rhyolite complex, Mexico. LCT: Lava Creek ash-flow tuff, Yellowstone. HRT: Huckleberry Ridge ash-flow tuff, Yellowstone (Hildreth, 1981). Modified from Baker and McBirney, 1985.

53

complete sections of the middle member in the northern Elkhorn Mountains (1962; 1966, p. 33), and 2) the fact that only the lower part of the middle member is present in the study area. However, a detailed study of field relations over a greater region of exposures of the Elkhorn Mountains Volcanics is needed to refine the number of ash-flow sheets present in the entire volcanic sequence.

The ash-flow sheets of the Elkhorn Mountains Volcanics are most similar to the "monotonous intermediates" of Hildreth (1981) (Figure 13) in terms of SiO_2 concentrations. Most major and trace elements show overall uniformity within the individual ash-flow sheets (Table 3). Likewise, in considering the system as a whole, the increases in concentration of the incompatible trace elements Cr, Hf, Ta, Zr, and Th (Figure 8) are consistent with those for other systems of intermediate composition (Baker and McBirney, 1985).

Smith (1979) and Hildreth (1981) have suggested that "monotonous intermediate" ash-flow sheets sample the dominant volume in magma chambers. If so, the eruption of ash-flow sheets with SiO_2 concentrations primarily between 58 and 69% in the Elkhorn Mountains Volcanics may simply reflect the fact that the system erupted before development of a highly silicic top.

The Lava Flows. The steep negative slopes of Ni, Cr, Sc, and Co against Th in the younger lavas (Figure 8) are consistent with a history dominated by crystal-liquid fractionation, either crystal fractionation or partial melting. Crystal fractionation of the sample (#3) of the least-evolved lava flow from the lava flow group VIII was modeled assuming equilibrium between the total crystallizing solid and melt. The expression

$$\frac{C_L}{C_i} + \frac{1}{F' + D_S (1 - F')} \qquad \text{(Arth, 1976)}$$

was used, where

C_L = trace element concentration of the differentiated liquid

C_i = trace element concentration of the original melt

Magma volume erupted
(km³)

BISHOP TUFF — 500
HUCKLEBERRY RIDGE — 2500
LAVA CREEK TUFF — • 1000

TSHIREGE —'—• • 300
FRACTION TUFF — 2500
RAINIER MESA • —...' 1000
AMMONIA TANKS — 800
TOPOPAH SPRING — — 250
TIVA CANYON • — 1000
APACHE SPRING — • 1400
CARPENTER RIDGE —'..• .500

MONOTONY TUFF — 3500
FISH CANYON TUFF '-— 3000
SNOWSHOE MOUNTAIN — 500

VTTS 1912 • — 15

SHIKOTSU — • 60
MAZAMA — — 50
ANIAKCHAK — — 35
KRAKATAU 1883 — • 10

FANTALE TUFF — • 2
LAACHER SEE —.... >5
FOGO A — 06

DEVINE CANYON • 250
TALA TUFF •• 20
GROUSE CANYON — • 200
SPEARHEAD —..—. 150

GRAN CANARIA P1 —.....—.—. >25
ASKJA 1875 — ....• .— 02
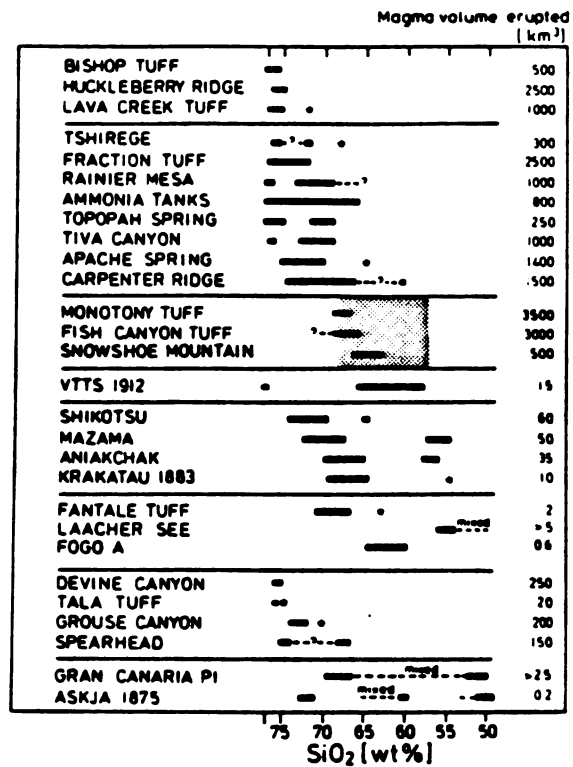
75 70 65 60 55 50
SiO₂ (wt%)

Figure 13. SiO$_2$ ranges of some selected eruptive units (after Hildreth, 1981, figure 1). Shaded area shows SiO$_2$ range of ash-flow sheets in the Elkhorn Mountains Volcanics superimposed on "monotonous intermediates" of Hildreth (1981).

F' = fraction of liquid remaining

D_S = bulk distribution coefficient, calculated from the weight fractions of each fractionating mineral (w) and its solid-liquid distribution coefficient (K_D); $D_S = \sum_{I=1}^{n} w_i K_{D_i}$ (Cox and others, 1979).

Partition coefficients for orogenic andesites were used in the modeling of sample #3 (see Table 4). As defined by Taylor (1969), orogenic andesites are typically hypersthene normative, containing 53-63% SiO_2, less than 1.75% TiO_2, and K_2O less than (0.145 x SiO_2). Table 2 shows that the SiO_2 and TiO_2 contents of the Elkhorn Mountains Volcanics lava samples meet these restrictions, except for sample 3, which contains just under 53% SiO_2. The potash abundances of samples 1, 5, 7, and 9 are less than the appropriate calculated value; the other measured K_2O contents are too high. Nonetheless, the choice of the distribution coefficients for orogenic andesites for modeling is reasonable, because of the probable mobility of K_2O discussed previously and because the samples otherwise meet the criteria. Modeling of separation of 33% olivine, 40% orthopyroxene, 20% magnetite, 5% plagioclase, and 2% clinopyroxene from lava #3 over 20% crystallization yields predicted trends of Ni, Cr, Sc, and Co that are in agreement with those of the actual concentrations in the rocks (Figure 14). The particularly good match of the predicted and actual Ni abundances and the partition coefficient of Ni in olivine (Table 4) suggest that olivine dominated the fractionation process.

Crystal fractionation in the younger lavas was further modeled using the method of Cox (1980). This quantitative procedure was designed for modeling major-element fractionation trends in basaltic rocks. The calculations yield values for the fraction of liquid remaining and the composition of the residual liquid, as well as the composition of olivine, plagioclase, and clinopyroxene in equilibrium with the liquid after specified intervals of fractionation.

56

Table 4. Partition coefficients used in modelling
(from Gill, 1978).

	Ni	Cr	Sc	Co
Olivine	12	2	.27	1.35
Orthopyroxene	4	2	3	6
Magnetite	8	2	2	8
Plagioclase	.04	13	.065	.049
Clinopyroxene	6	30	3	2
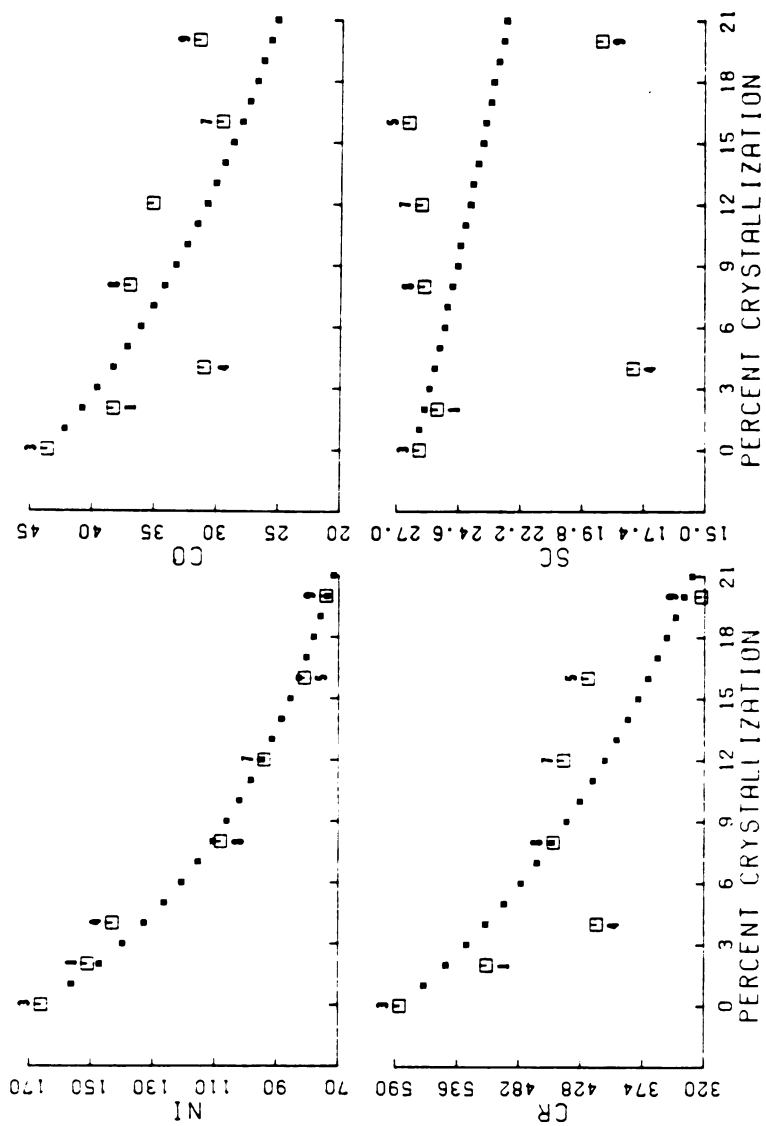
Figure 14. Results of modeling: Predicted and actual values of Ni, Cr, Sc, and Co in lava groups V and VIII. Modeling of fractional crystallization of olivine, clinopyroxene, magnetite, and plagioclase over 20% crystallization of lava #3 resulted in the plotted % crystallization and predicted trace element concentrations (*); best fit actual values of trace element concentrations (open squares) were superimposed on this curve. Sample numbers indicated correspond to Table 2.

Fractionation of lava sample 3 was modeled over 20% crystallization of the starting composition. Because this method allows modeling of only olivine, plagioclase, and clinopyroxene, the same relative proportions of those minerals were used as those that produced the best agreement of predicted and actual trace element trends (i.e., 33% olivine, 5% plagioclase, and 2% clinopyroxene were normalized to 100% and became 82.5% olivine, 12.5% plagioclase, and 5% clinopyroxene). This approach is plainly idealized, and absolute agreement between the predicted and actual major-element concentrations would not be expected. However, reasonably similar trends in predicted and actual Mg* (Mg/Mg + Fe) were found (Table 5); this is good support for the possibility that fractionation in the younger lavas is dominated by olivine.

Processes Common to Both the Ash-flow Sheets and the Lava Flows. The Eu/Eu* values provide further evidence for fractionation of the Elkhorn Mountains Volcanics (Figure 15). As discussed earlier, the Elkhorn Mountains Volcanics have only slight or no Eu anomalies. For most of the lava flow samples, the values of Eu/Eu* lie between 0.9 and 1.0, indicating at best only minor plagioclase fractionation. Two lava flow samples with Eu/Eu* greater than 1 apparently evolved by addition of plagioclase-composition crystals or melt. In the ash-flow sheet samples, however, there is significant plagioclase fractionation which increases with increasing differentiation of the liquids. This interpretation is also supported by the trend seen in Eu/Eu* against Sr (Figure 15).

In contrast, there is no evidence of alkali feldspar fractionation in either the lava flows or the ash-flow sheets. Increasing Ba abundances in a suite of differentiated, cogenetic rocks indicate no fractionation of alkali feldspar (Baker and McBirney, 1985) (Figure 8). Similarly, decreasing Sr can be explained by fractionation of plagioclase (Figure 8), already indicated by the Eu/Eu* values (Figure 15).

Table 5. Trends in actual and modeled Mg*.

|	Fo	Di	An
Starting compositions: LAVA #3			
Mg* (liquid) = Mg/(Mg + Fe) = 78.62			
Calculated equilibrium mineral compositions:	92.4	95.3	72.8
Step 1: 95% liquid remaining			
Mg* (liquid) = 75.79	91.2	94.5	73.2
Step 2: 90.25% liquid remaining			
Mg* (liquid) = 72.08	89.2	93.5	73.5
Step 3: 85.74% liquid remaining			
Mg* (liquid) = 67.00	87.1	91.8	73.8
Step 4: 81.45% liquid remaining			
Mg* (liquid) = 59.38	83.0	89.0	74.2
Final composition: LAVA #6			
Mg* = 67.01			
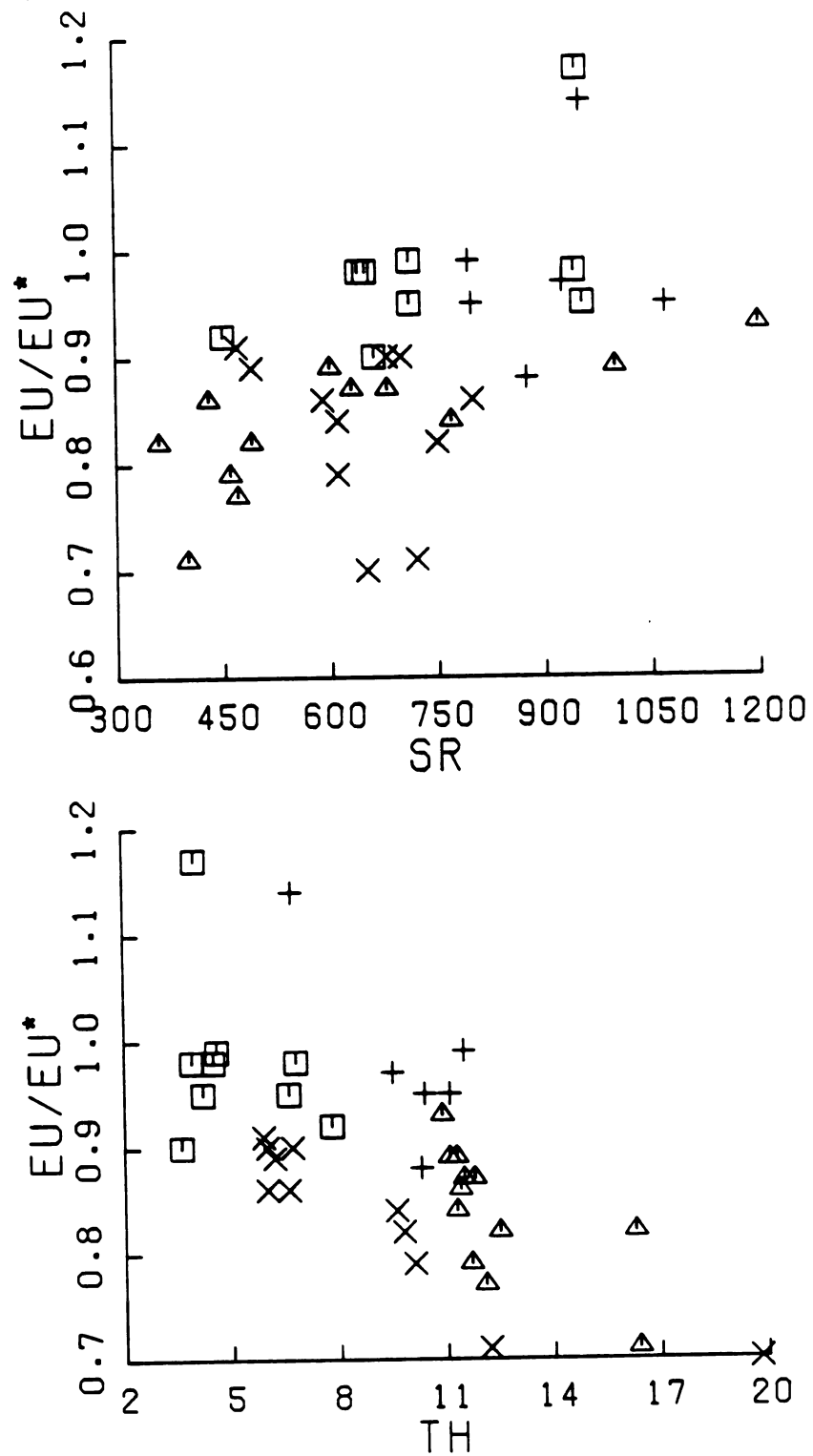
Figure 15. Plots of Eu/Eu* against Th and Sr for The Elkhorn Mountain Volcanics. Symbols as in Figure 5.

Possible Relationships Among the Lava Flows and the Ash-flow Sheets

Two separate trends in plots of SiO_2, MgO, and Fe as Fe_2O_3 against Th (Figure 16) suggest two lines of evolution among the lava flows and ash-flow sheets in the study area. The fields outlined in Figure 16 show lava flow groups V and VIII leading to ash-flow sheet IV and VII and lava flow group II leading to the other ash-flow sheets, except I. Both lines follow increasing differentiation as defined by Th. Similar pairing is observed in the variation of Ce, Hf, Ta, and Zr with Th (Figure 8).

Neither possible evolutionary path can be explained by crystal-liquid fractionation. Attempts to model fractionation from each lava group to the corresponding ash-flow sheets were not successful.

The possibility of magma mixing being the dominant mechanism has been evaluated using ratio-ratio plots (Figure 17). Ideally, in Figure 17a, if either lava flow - ash-flow sheet(s) pair is genetically related by magma mixing, the samples should plot on hyperbolic curves. The permissibility of mixing as a viable process in the evolution from the lava flows to the ash-flow sheets can be supported further if the samples lie on straight lines in Figure 17b. Two possible positions of hyperbolae and straight lines are shown between the suggested lava flow - ash-flow sheets pairs in Figure 17. From examination of Figure 17, it is concluded that simple magma mixing was not a dominant process, although some mixing may have taken place.

The failure of both fractionation and magma mixing to dominate the processes producing the chemical changes from the lavas to the ash-flow sheets implies that the apparent relationships are the results of a combination of evolutionary mechanisms, not of any single process. The entire system was almost certainly a dynamic one, evolving by a combination of mechanisms while receiving injections of new magma at intervals and, just as periodically, losing

Figure 16. Plots of SiO_2, MgO, and Fe as Fe_2O_3 against Th. Dashes outline field of lava groups V and VIII and ash-flow sheets IV and VII. Solid line outlines field of lava group II and all other ash-flow sheets except I. Symbols as in Figure 5.
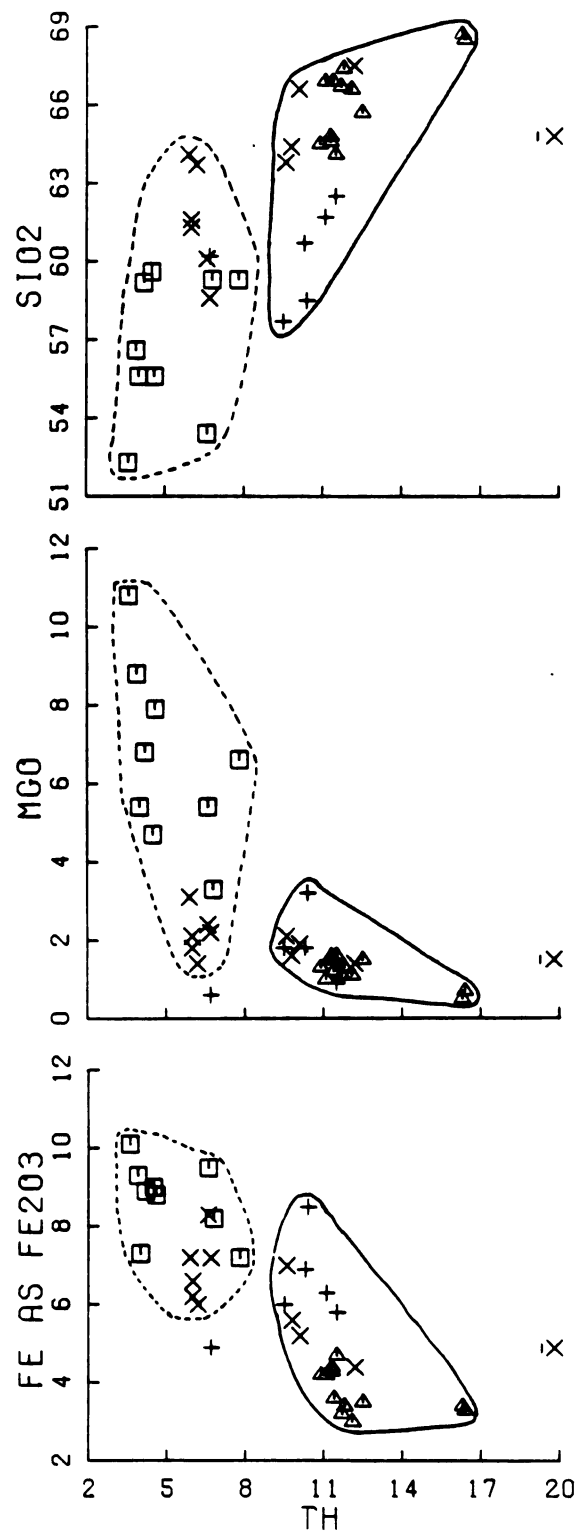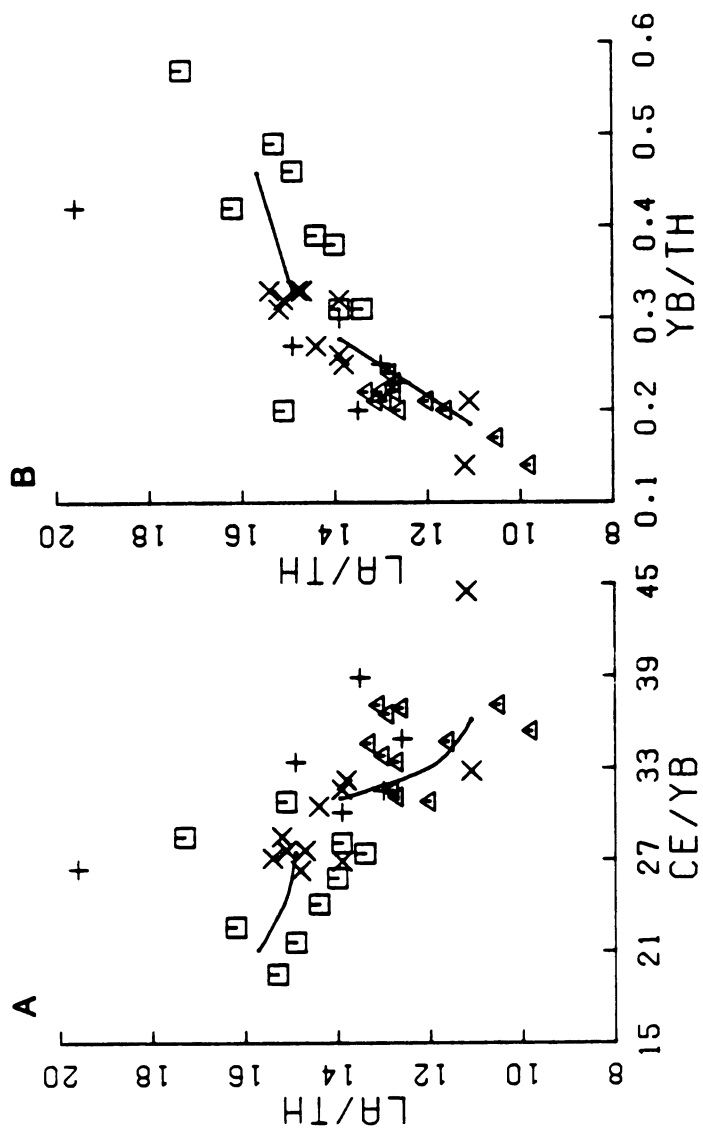
Figure 16.

Figure 17. Ratio-ratio plots to evaluate role of magma mixing. A) La/Th against Ce/Yb. B) La/Th against Yb/Th. Lines in (A) and curves in (B) show possible magma mixing relationships between lava groups V and VIII and ash-flow sheets IV and VII and lava group II and lava group VII and ash-flow sheets VI and those in the middle member. Symbols as in Figure 5.

various volumes in lava and ash flow eruptions. Possibly both crystal fractionation and magma mixing had minor roles in producing the chemical trends. In a magmatic system of this size, convection and diffusion would be expected and could play a major role (Smith, 1979; Huppert and Sparks, 1984). Influx of new material and eruption of evolved ash flows were most likely periodic through the early stages of the system. During this early period of evolution, thermal flux was high and crystallization was limited. The only demonstrable crystal fractionation was of olivine. This high thermal flux was due to and maintained by influxes of relatively primitive magma. Later in the volcanic phase, evolution of the magmatic system by fractionation of plagioclase feldspar occurred.

The Evolution of the Entire Magmatic System within the Time Frame Represented in the Study Area

The evolution of the Elkhorn Mountains Volcanics over the period of time represented by these lava flow samples and ash-flow sheet samples may be evaluated in terms of both caldera cycles (Christiansen, 1979) and models for evolution of high-level magmatic systems (Smith, 1979; Hildreth, 1981) and by comparison with other ash-flow fields of similar size.

Interpretation of Caldera Cycle Remnants. It has long been established that eruptions of ash-flow tuffs are commonly associated with caldera collapse (Williams, 1941; Smith, 1960) and that many calderas have histories of repeated eruption and collapse. Christiansen (1979) summarized the basically similar sequence of events in several examples. Is it possible to identify aspects of such cycles in this sequence of the Elkhorn Mountains Volcanics and to relate them even in a general way to their possible caldera-source areas?

A summary of the changes in chemistry in the Elkhorn Mountains Volcanics in terms of the variation of Th abundances with time (Figure 18) provides a reasonable tool with which to begin answering this question. All of the samples
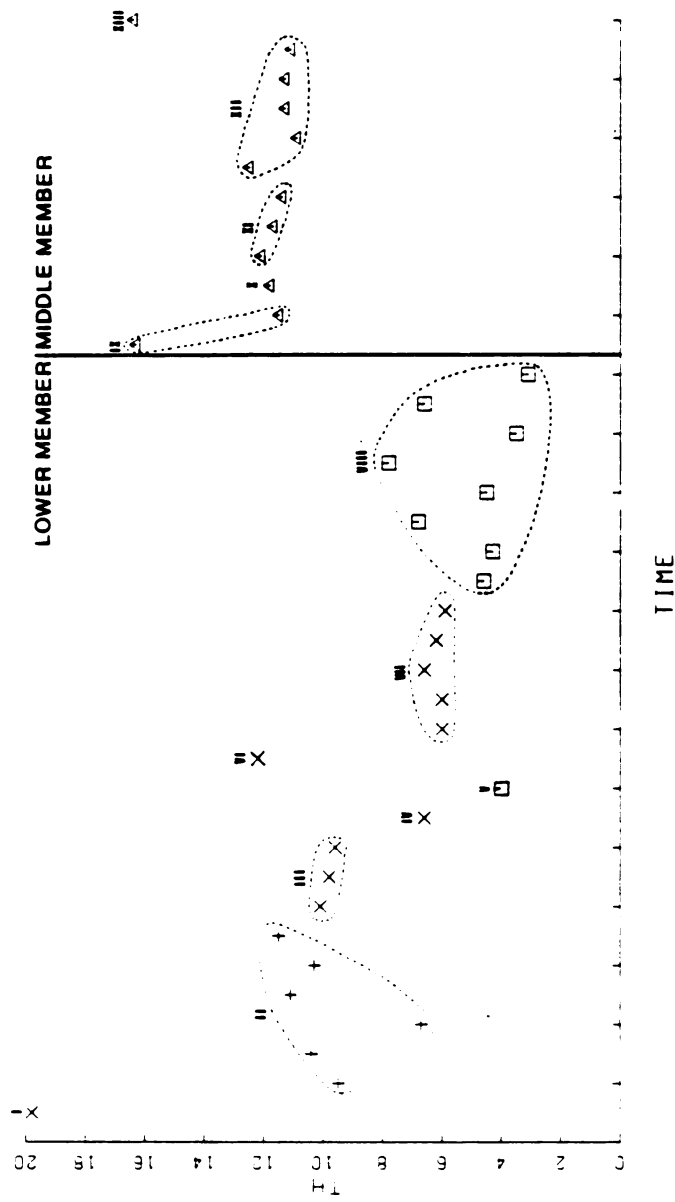
Figure 18. Plot of Th against time. Samples are arbitrarily spaced at regular intervals along the time axis. Symbols as in Figure 5.

are arbitrarily spaced at regular intervals along the time axis because their exact ages are not known; however, crosscutting field relations and K-Ar age determinations of the volcanic and plutonic rocks indicate that the volcanic activity which produced the lower and middle members took place over 2-3 million years, from about 81 to 76 Ma ago (Tilling, 1973, 1974). The following discussion is based on Figure 18.

The variation of Th with time for units of the lower member, composed of intercalated lava flows and ash-flow sheets (Figure 4), may provide a fragmental record of several caldera cycles. Ash-flow sheet I is likely the product of a caldera-forming event early in the history of the Elkhorn Mountains Volcanics; it is interpreted to be the base of an ash flow sheet whose upper thickness was eroded prior to eruption of the older group of lava flows (II). Lava flow group II may be pre-caldera lavas to some later ash flow eruption, perhaps represented by ash-flow sheet III, VI, or the sequence in the middle member (ash-flow sheets IX through XIII); all of these possibilities could be argued on chemical grounds in view of the trends in Figure 16. Many chemical aspects of ash-flow sheet IV are similar to those of sheet VII (see Figure 16, for example); this similarity could indicate that sheet IV is a product of an eruption from the same source/chamber that later produced sheet VII. The best preserved cycle in the lower member is probably the caldera-forming eruption of ash-flow sheet VII; the possible relationship between this sheet and lava flow group VIII suggests that they are post-caldera lavas associated with this event. Lava flow V precedes ash-flow sheet VII in time and could be a remnant of the pre-caldera lavas of this cycle.

The ash-flow sheets in the middle member (IX through XIII) are each separated from the next-younger sheet by some significant physical break (see Figure 4). However, many aspects of their chemistry are quite uniform and similar (note the clustering of analyses L through C in Figure 16, for example).

68

The most highly differentiated samples, M and A, come from the bases of ash-flow sheets IX and XIII, respectively. Thus, ash-flow sheets IX through XII may be considered products of a single catastrophic eruptive episode, a complex one that might have tapped several separate culminations above the larger magma chamber. According to this interpretation, ash-flow sheet XIII would then represent the base of another, perhaps also complex, ash- flow sheet.

Comparison of the Elkhorn Mountains Volcanics to the Similar-Sized Timber Mountain and Associated Calderas Complex. The interpretation of the caldera cycles in the Elkhorn Mountains Volcanics (Figure 18) can be more complete by comparing these cycles to those of a system of comparable size whose volcanic history is better preserved. The Timber Mountain and associated calderas complex in southern Nevada is suitable for such an analogy. This caldera complex occupies an area of roughly the same dimensions as those of the Boulder batholith, which presumably reflect the pre-erosional extent of the nested suite of calderas related to the eruption of the ash-flow sheets of the Elkhorn Mountains Volcanics. The study area may thus be compared to the region outlined in the map of the Timber Mountain and associated calderas complex in Figure 19.

Over a time span of about 5 Ma, between 16 and 6 Ma ago, the Timber Mountain and associated calderas complex developed 4 to 6 calderas. Each caldera formed concurrently with the eruption of 1 to 3 predominantly rhyolitic ash-flow sheets, resulting in at least 14 ash-flow sheets plus other rhyolitic tuffs and lava flows; estimated erupted volumes of the ash-flow sheets range from 20 to over 1200 km^3 (Christiansen and others, 1977; Scott and others, 1984). The Elkhorn Mountains Volcanics and the Timber Mountain and associated calderas complex have approximately the same areal extent; with respect to time span of volcanic activity and number of calderas and ash-flow sheets, they may also be similar.
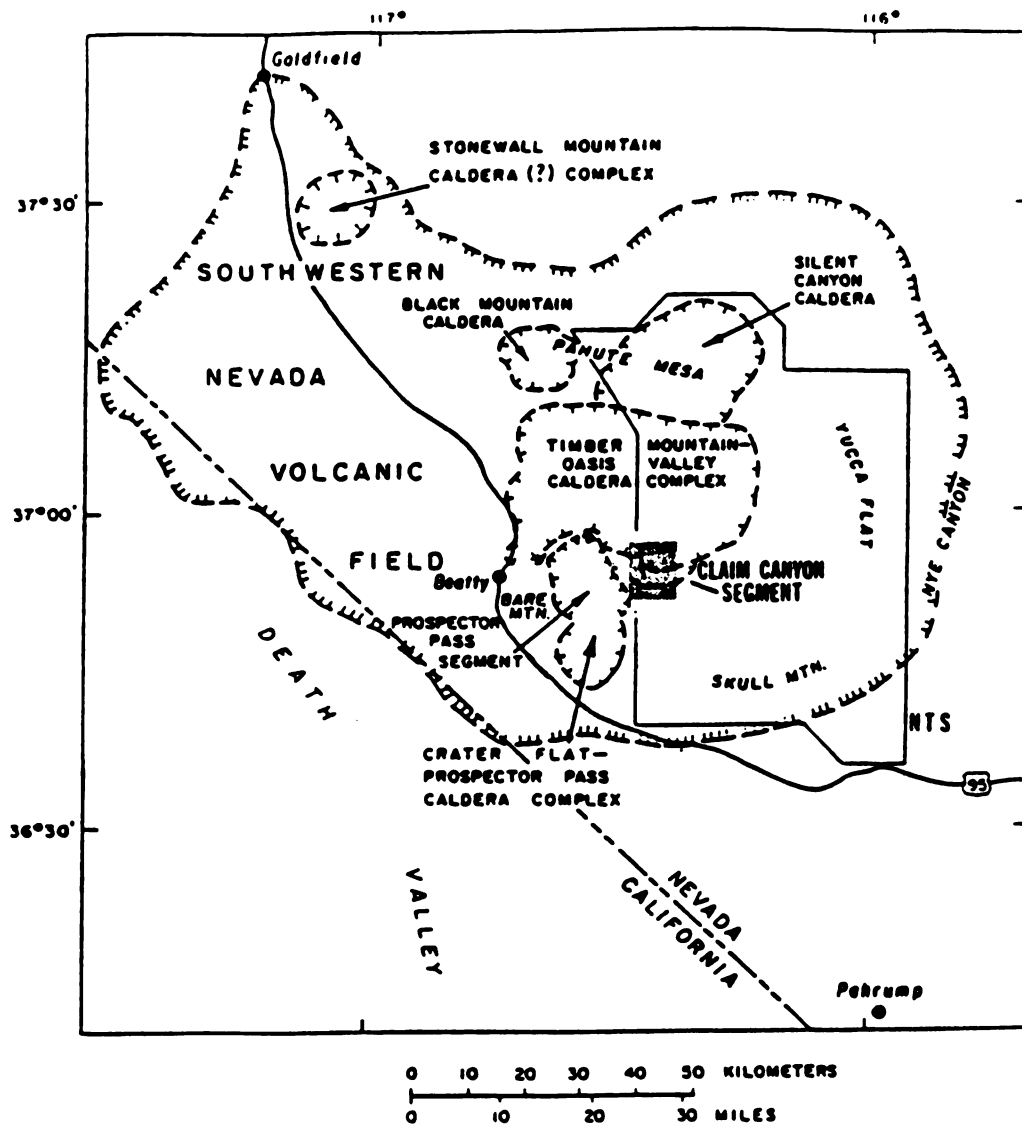
Figure 19. Map of the Timber Mountain and related calderas complex (after Carr and others, 1985). Stippled area shows region analogous to Elkhorn Mountain Volcanics study area.

70

Based on the caldera cycles in the Timber Mountain and associated calderas complex (Byers and others, 1976), a possible pre-erosion scenario for the Elkhorn Mountains Volcanics preserved in the study area can be constructed (Figure 20). The sequence of events represented in these highly schematic cross sections begins after the eruption of ash-flow sheets I, III, and IV and lava flows II and V on eroded Cretaceous sedimentary rocks. Caldera formation related to eruption of these ash-flows probably took place to the west (Figure 20-1). Subsequence to these events, eruption of ash-flow sheet VII and caldera collapse took place, followed by eruption of lava flow group VIII (Figure 20-2). Figure 20-3 illustrates the possible configuration of the units at the start of eruption of the ash-flow sheets in the middle member and associated caldera formation. The final schematic cross-section in this series shows possible resurgence of an early middle member caldera (Figure 20-4).

Comparison of the Elkhorn Mountains Volcanics to the Boulder Batholith

The Elkhorn Mountains Volcanics are coeval with the associated plutons of the Boulder batholith (Robinson and others, 1968; Klepper and others, 1957; Smedes, 1966; Doe and others, 1968; and Tilling, 1973, 1974). The chemical analyses from this study may be compared to analyses of the associated plutonic rocks in an attempt to improve the present understanding of the relationship between the batholith and the volcanics. A further goal of this comparison is to contrast the fractionation processes which influenced the evolution of the volcanics with those which influenced evolution of the plutonics. It is important to realize that the plutonic rocks represent crystallized products and not magma, whereas the volcanic rocks are direct samples of the magma. In volcanic rocks, the processes that control the evolution of the magma can be directly inferred rather than having to interpret the magmatic processes from the crystallized product.
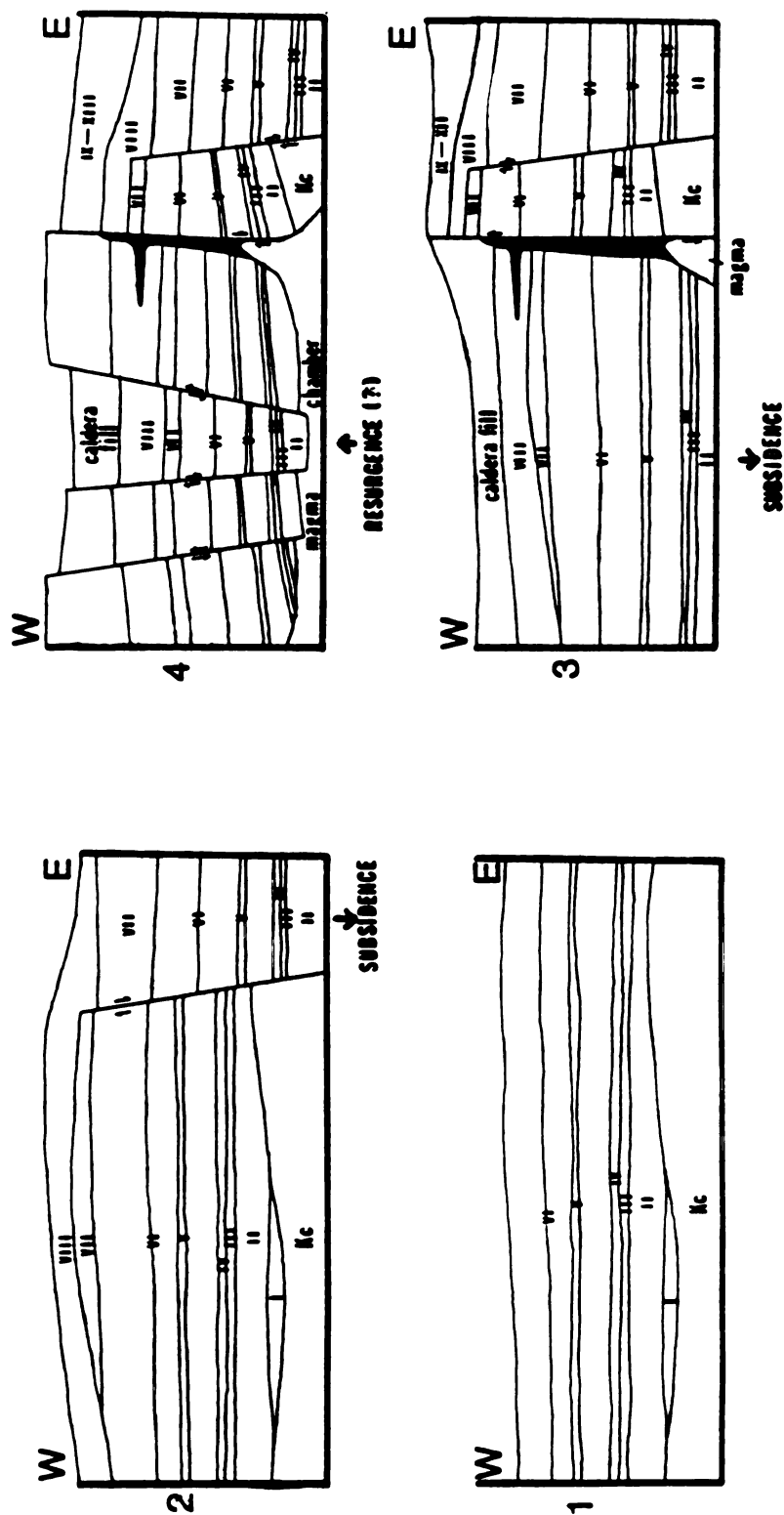
71

Figure 20. Highly schematic sequence of pre-erosion Elkhorn Mountain Volcanics cross-sections based on Timber Mountain and related calderas complex analogy (after Byers and others, 1976). Roman numerals correspond to units labeled in Figure 4; unlabeled units correspond to lithologies in Figure 4.

Tilling (1973) recognized and defined two magma series in the batholith, the main series and the sodic series. Rocks from the main series contain more K_2O and less Na_2O at a given SiO_2 content than do rocks from the sodic series. Because of mobility of K_2O, Na_2O, CaO and related trace elements recognized in the Elkhorn Mountains Volcanics, comparison of the volcanic and the plutonic rocks is necessarily limited, and such limitation should be considered in the following discussion.

The Elkhorn Mountains Volcanics analyzed in this study show great similarity to the main series plutons when plotted in a K_2O-Na_2O-CaO diagram (Figure 21). This affinity of the Elkhorn Mountains Volcanics for the main series agrees with the conclusion of Tilling (1973, 1974) that the volcanics are compositionally more like the main series than the sodic series.

Tilling (1973) found that the variation of Rb and Sr with respect to SiO_2 also could be used to illustrate the two magma series. The distribution of Rb in the Elkhorn Mountains Volcanics is similar to that in the main series; the scatter in the distribution of Sr, which obscures any affinity of the volcanics for either series, is probably due to mobility (Figure 22).

The abundances of Nb, Y, Zr, Pb, Cu, and Ba in the plutons of the southern portion of the Boulder batholith were determined by Lambe (1981) in order to further confirm and characterize the two magma series. The new analyses of Y, Cu, Zr, and Ba are plotted with Lambe's (1981) data in Figure 23 against SiO_2. Yttrium distribution is relatively constant in both the volcanics and the batholith and does not distinguish either magma series in any respect. Copper in the lava flows falls rapidly as SiO_2 increases; the same pattern is seen in the plutonic main series, in contrast to the sodic series, where Cu is fairly constant. Zirconium in the volcanics shows neither the rapid depletion of the main series nor the uniformity of the sodic series observed by Lambe (1981); it exhibits a much wider

73
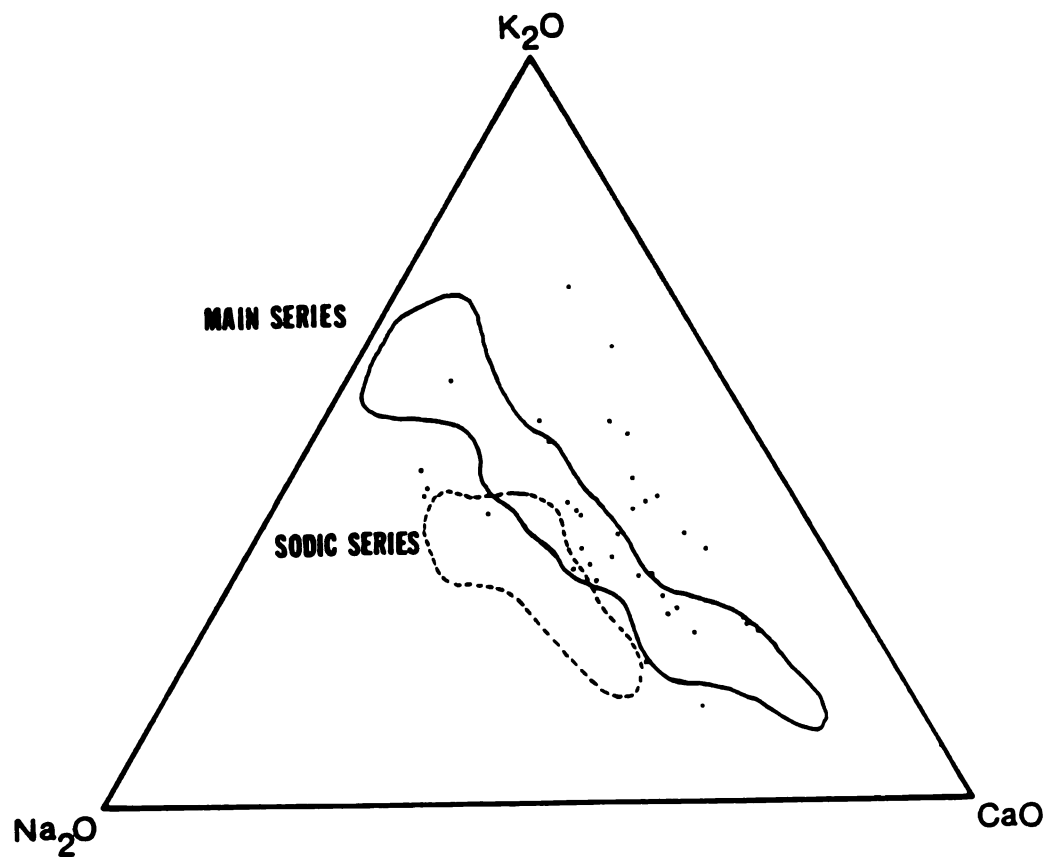
Figure 21. K_2O-Na_2O-CaO diagram of the two plutonic main and sodic series fields and the Elkhorn Mountains Volcanics (solid circles) (modified from Tilling, 1973; volcanic data from Tables 2 and 3).

Figure 22. Plots of Rb and Sr against SiO$_2$ in the Elkhorn Mountains Volcanics and the plutonic main and sodic series fields (modified from Tilling, 1973). Symbols as in Figure 5.

Figure 22.

76
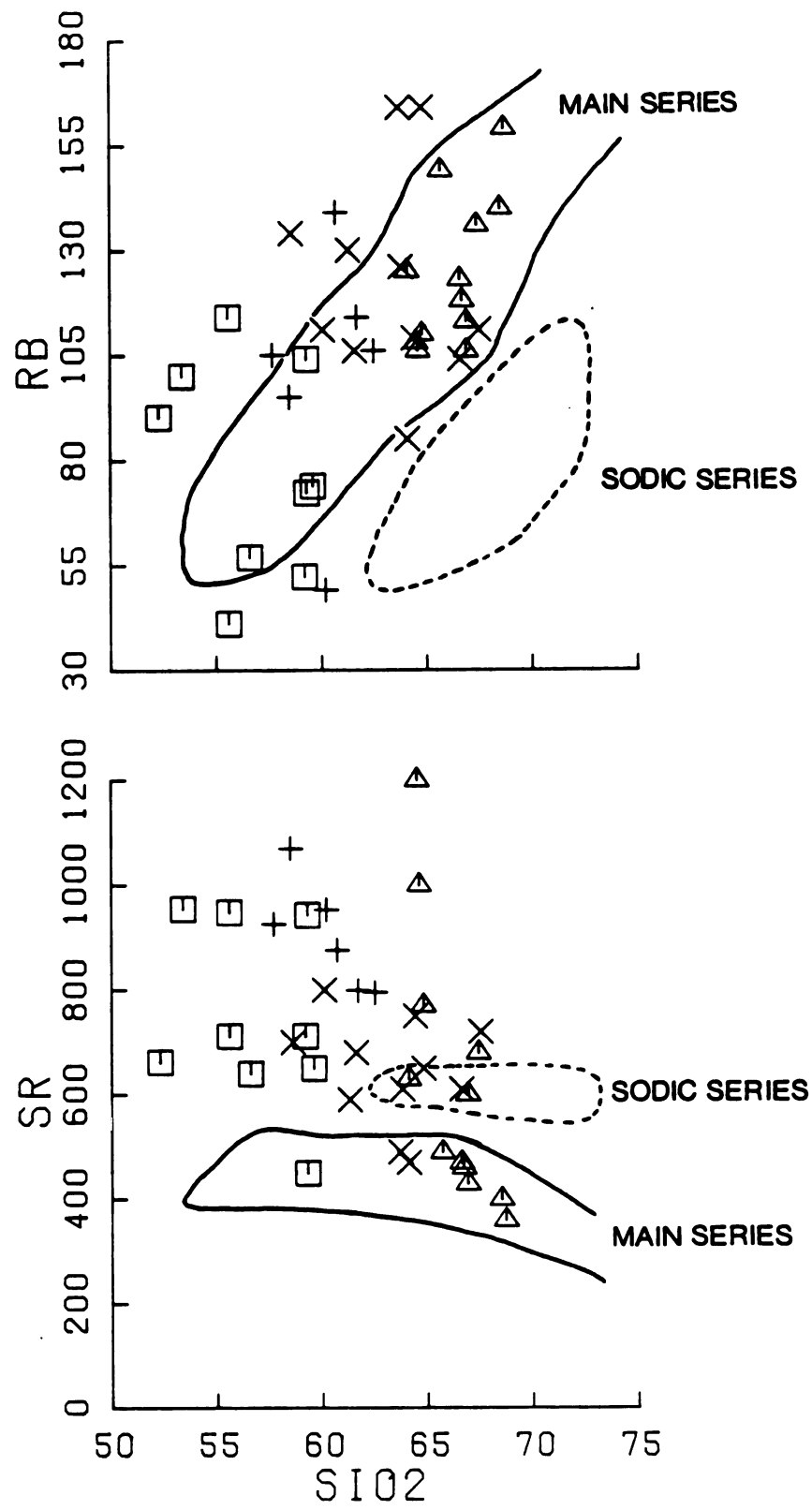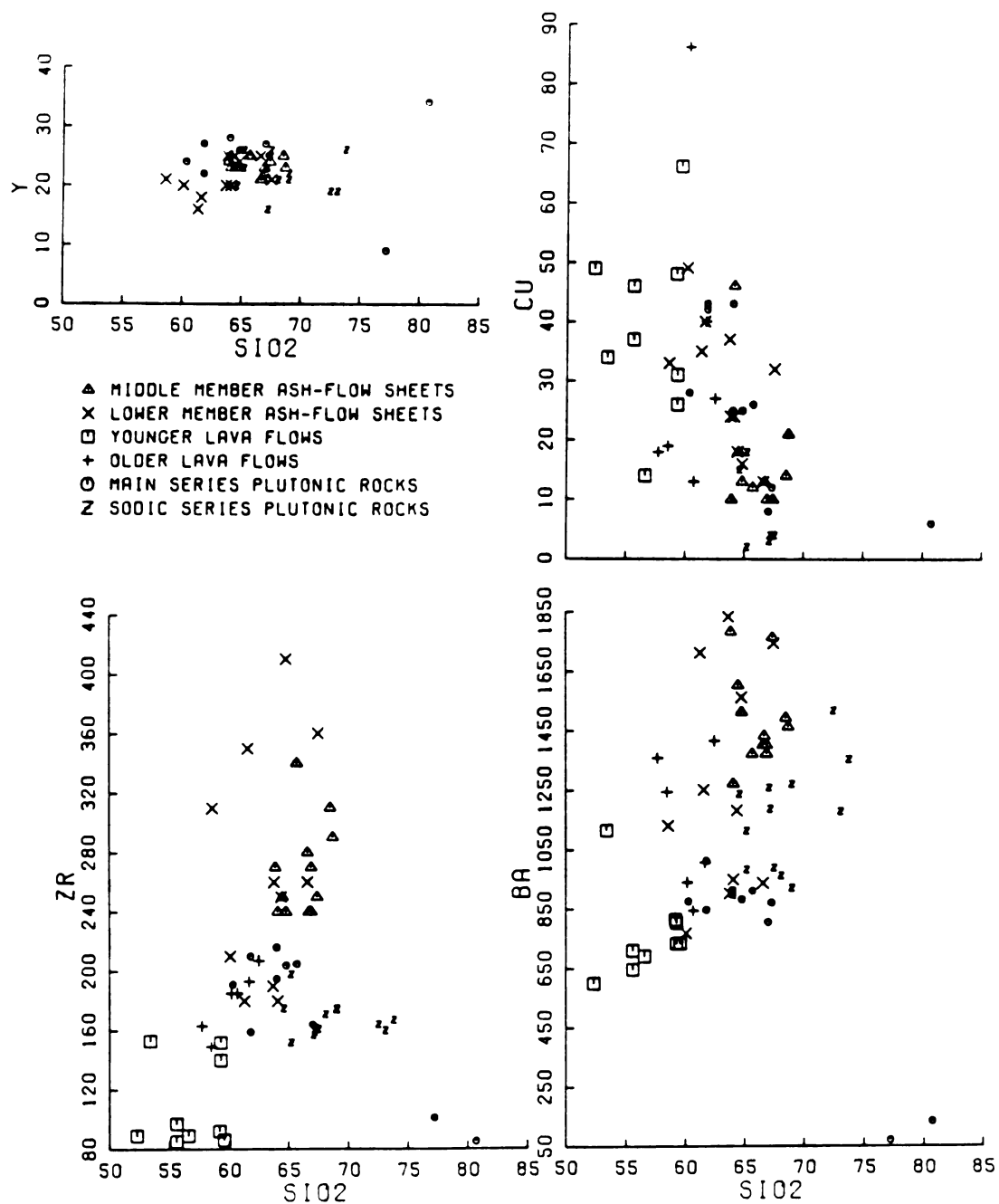
Figure 23. Abundances of Y, Cu, Zr, and Ba in the Elkhorn Mountain Volcanics and the plutons of the southern part of the Boulder batholith (plutonic data of Lambe, 1981) in plots against SiO_2.

range of values in the volcanics and correlates positively with increasing SiO_2. The positive trend of Ba abundances in the volcanic rocks parallels a similar trend in the sodic series. This trend in the volcanic rocks has already been explained as indicating no fractionation of alkali feldspar. Lambe (1981) attributed Ba enrichment in the sodic series to late crystallization of alkali feldspar and Ba depletion in the main series to possibly early crystallization of biotite. The Ba abundances are thus indicative of processes which influenced the evolution of the volcanic and plutonic rocks, not of any trace element signature of either plutonic series or of the volcanic rocks.

Lambe (1981) also presented chondrite-normalized REE profiles for the main and sodic series. In comparison with the REE profiles of the volcanics (Figure 10), the plutonic rocks show pronounced negative Eu anomalies (Figure 24). Eu/Eu* can be calculated for only two of Lambe's samples, one from the Butte Quartz Monzonite and the other from the Burton Park pluton; his other samples contain no detectable Tb. Eu/Eu* for the Boulder batholith are presented in Table 6 with Eu/Eu* calculated for the volcanics; all Eu/Eu* are plotted against Th in Figure 25. The Eu anomalies in the plutonic rocks are clearly more negative than in the volcanic rocks, two of which exhibit slightly positive anomalies. The large negative Eu anomalies in the plutonic rocks suggest that plagioclase fractionation played a significant role in the evolution of the batholith. In contrast, the evolution of the volcanics seems to have been only slightly, if at all, controlled by plagioclase fractionation.

The strongly incompatible behavior of Zr in the volcanics (Figures 8 and 23) implies that no fractionation of zircon occurred. The likewise incompatible behavior of Hf (Figure 8) supports this conclusion. In contrast, the decrease in Zr with increasing SiO_2 in the plutonic main series (Figure 23) is best explained by crystallization of zircon (Lambe, 1981). An important influence on Zr abundance

Table 6. Eu/Eu* in the Boulder batholith and the Elkhorn Mountains Volcanics.

Sample Number	Eu/Eu*
Plutonics[1]	
701-8	.607
483	.503
Ash-flow Sheets[2]	
A	.706
C	.894
D	.887
E	.837
F	.931
G	.817
H	.861
I	.789
J	.772
K	.867
L	.869
M	.816
N	.906
O	.888
P	.904
Q	.896
R	.864
S	.708
T	.856
U	.842
V	.823
W	.789
X	.703
Lavas[3]	
1	.978
2	.951
3	.903
4	.918
5	.978
6	.977
7	.953
8	.991
9	1.17
10	.991
11	.878
12	.946
13	1.14
14	.953
15	.967

1 = Data of Lambe, 1981.
2 = Data of Table 3.
3 = Data of Table 2.

Figure 24. Chondrite-normalized rare earth element profiles for the Boulder batholith (from Lambe, 1981).
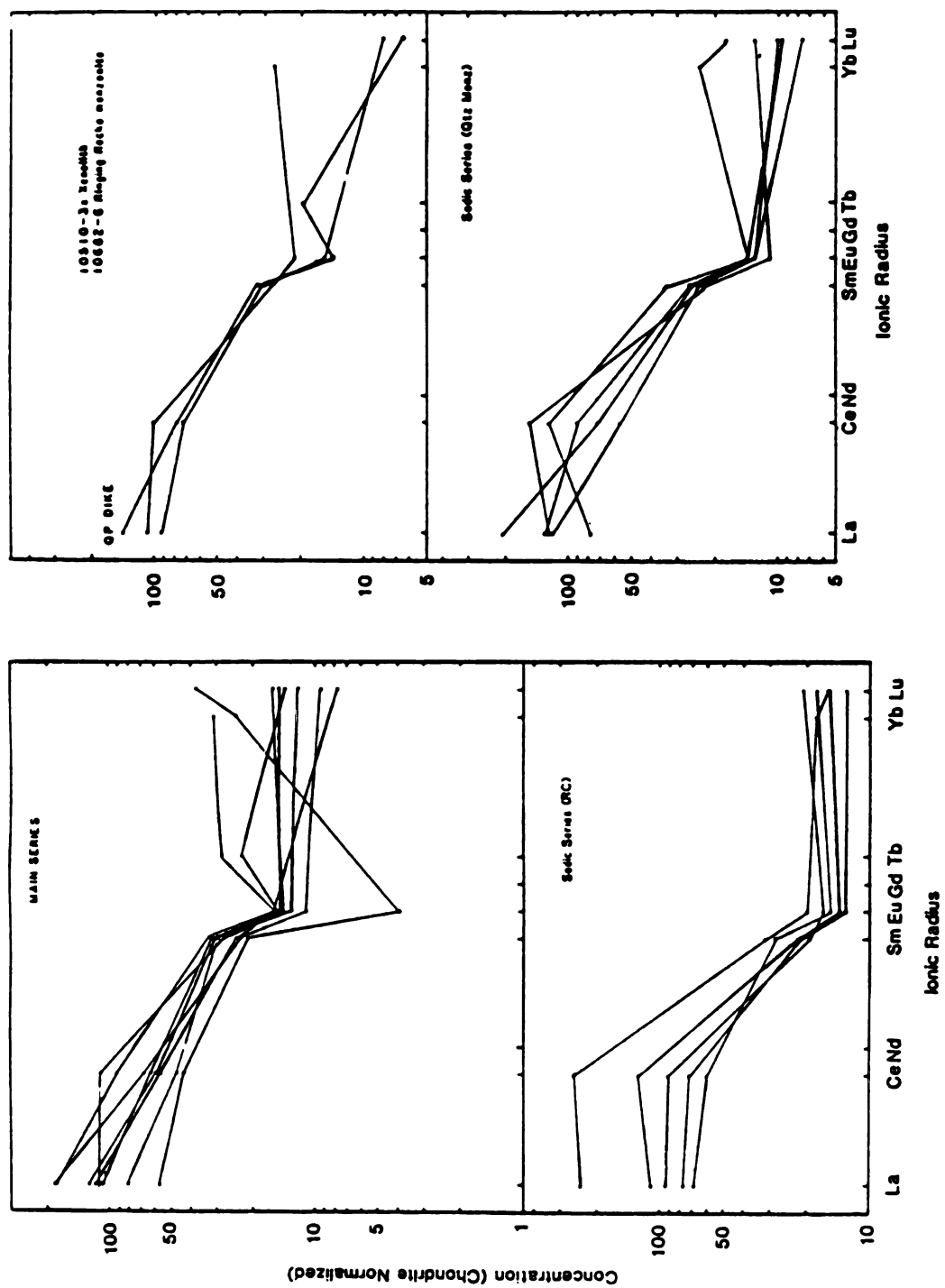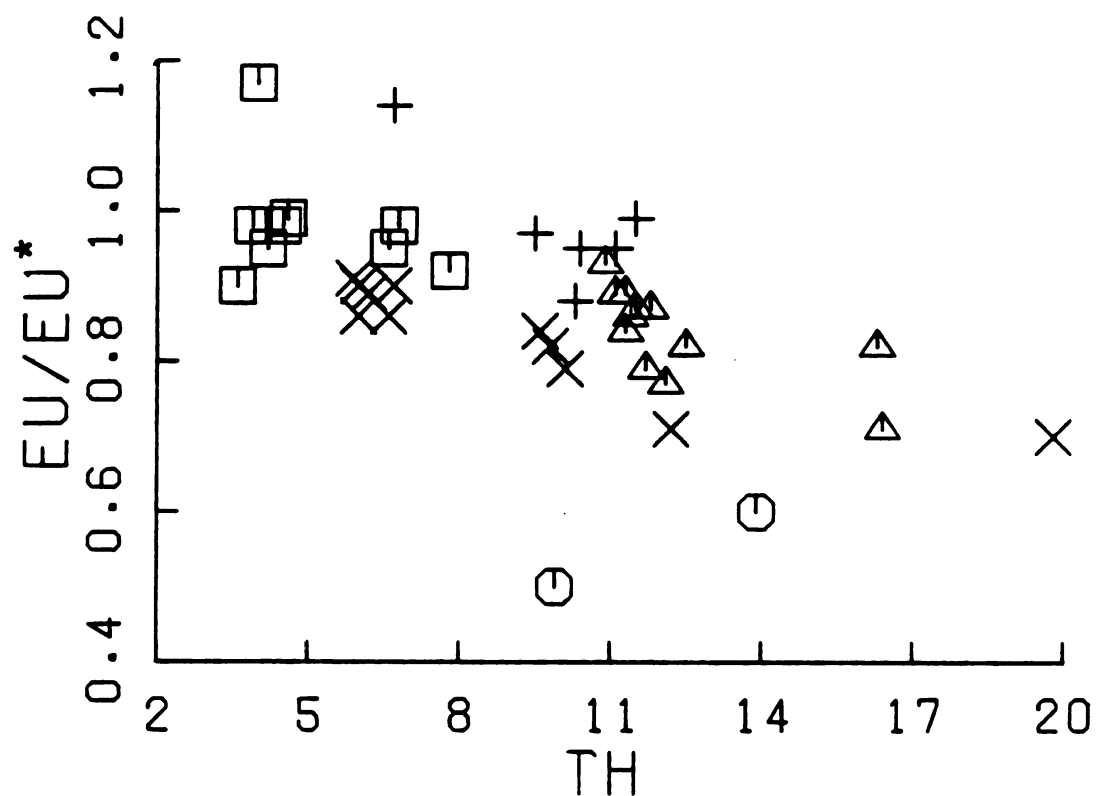
Figure 24.

81

Figure 25. Plot of Eu/Eu* against Th for the Elkhorn Mountains Volcanics and the Boulder batholith (batholith data from Lambe, 1981).

is seen in the experimental data of Watson (1979), that demonstrate a direct relationship between Zr solubility and rock alkalinity. Watson (1979, p. 415) states that "only two variables are of major importance in determining whether a magma is saturated in zircon: 1) the amount of Zr present in the system, and 2) the $(Na_2O + K_2O)/Al_2O_3$ ratio of the liquid." For compositions in which this ratio is less than or equal to 1.0, zircon becomes saturated in the melt at less than 100 ppm; for values greater than 1.0, Zr solubility increases linearly from 100 ppm at $(Na_2O + K_2O)/Al_2O_3 = 1.0$ to almost 4 wt % at $(Na_2O + K_2O)/Al_2O_3 = 2.0$. From the Zr abundances and $(Na_2O + K_2O)/Al_2O_3$ ratios given in Table 7 for the Elkhorn Mountains Volcanics, it is clear that the "peraluminous" ash-flow sheet samples contain more Zr than should be possible based on experimental data. This inconsistency is best explained by mobility loss of K_2O, which has been previously discussed. Because the present $(Na_2O + K_2O)/Al_2O_3$ in the volcanics almost certainly do not reflect the original ratios and because most of the samples contain over 100 ppm Zr, it is likely that the parent magma for the Elkhorn Mountains Volcanics was peralkaline.

Comparison of Volcanic and Plutonic Processes

The conclusion that the volcanic and plutonic rocks evolved along different paths is supported by the evidence for crystal fractionation. The Eu anomalies in the plutonic and the volcanic rocks indicate that crystal fractionation of feldspar was important during the development of the plutonic rocks, but was minor in the evolution of the volcanic rocks (Figure 25). Although chemical modeling has permitted the argument for crystal fractionation of olivine in the volcanic rocks (Figure 13), the role played by this process was not a prominent one and apparently influenced only the early stages of evolution of part of the magmatic system.

Table 7. Zr and $(Na_2O + K_2O)/Al_2O_3$.

Lavas	$(Na_2O+K_2O)/Al_2O_3$	Zr ppm	
1	1.20	89	
2	1.22	153	
3	1.22	89	
4	1.23	152	
5	1.18	86	
6	1.22	140	
7	1.21	92	
8	1.22	97	
9	1.18	85	
10	1.28	207	
11	1.09	185	
12	1.12	193	
13	1.24	185	
14	1.22	149	
15	1.18	163	Range: 85-207

Ash-flow sheets

A	.55	310	
C	.23	240	
D	.31	270	
E	.44	240	
F	.33	250	
G	.38	340	
H	.38	270	
I	.28	240	
J	.39	280	
K	.50	250	
L	.46	240	
M	.29	290	
N	.45	180	
O	.49	190	
P	.57	310	
Q	.44	350	
R	.44	180	
S	.32	360	
T	.43	210	
U	.53	260	
V	.39	250	
W	.39	260	
X	.23	410	Range: 180-410

Analytical data from Tables 2 and 3.

The fact that at best minor amounts of feldspar fractionation occurred in the development of the Elkhorn Mountains Volcanics suggests that feldspar was unstable in the source region. Such a conclusion would be consistent with the lower crustal or upper mantle source model proposed by Doe and others (1968) to explain the isotope variations in the Boulder batholith, and with the genetic relationship between the batholith and the Elkhorn Mountains Volcanics.

The lower crust might thus have been the site of partial melting to produce the volcanic magmas, which were then emplaced and stored at shallow crystal levels. Minor fractionation of olivine and plagioclase, and perhaps pyroxene, and magnetite occurred. If magma mixing took place, perhaps in response ⁺

replenishment of the magma chamber(s) by partial melts, its e

The plutonic phase of the magmatic system was initiated as cry

upper portions of the magma system continued and the liquids ev

too viscous to erupt (Smith, 1979; Marsh, 1981)

CONCLUSIONS

The goals of this project were:

1) To identify the major processes that led to the chemical diversity of the Elkhorn Mountains Volcanics, based on interpretation of the major and trace element variations within the volcanics, and

2) To compare the evolutionary processes inferred from the volcanic rocks with those recorded in the plutonic rocks.

These goals have been accomplished in the conclusions summarized below.

Interpretation of the chemical trends within the Elkhorn Mountains Volcanics has shown that 1) some fractionation, primarily of olivine, influenced the evolution of lava flow groups VIII and V, 2) a small amount of fractionation of plagioclase occurred in the evolution of the ash-flow sheets - more occurred in the lava flows, and 3) no fractionation of alkali feldspar occurred.

The relationships among the lava flows and ash-flow sheets were not dominated by either crystal-liquid fractionation or magma mixing; a combination of these mechanisms, aided by convection and diffusion, may have occurred.

The chemical trends of the incompatible trace elements within the complete volcanic section are consistent with the conclusion that all of the Elkhorn Mountains Volcanics were related by evolution of a single magmatic system. The magmatic system envisioned consisted of several separately evolving magma bodies of combined batholithic dimensions, tapped at different depths and locations to produce the lava flows and ash-flow sheets of the Elkhorn Mountains Volcanics. The absence of zoning in the ash-flow sheets is interpreted as indicating that eruption occurred before development of a highly silicic upper zone in the magma chamber.

The Elkhorn Mountains Volcanics are similar to the main series of the Boulder batholith in K_2O, CaO, Na_2O, and Rb contents. This affinity is consistent with Tilling's (1973, 1974) conclusions that the volcanic rocks are more closely related to the main plutonic series than to the sodic series and that the plutons of the main series evolved from the magma left in the system after each volcanic withdrawal.

That the volcanic and plutonic rocks nonetheless evolved along different paths is plain from the available evidence. The plutonic phase, as represented by the Boulder batholith, appears to have been affected more by feldspar fractionation. In contrast, very little feldspar fractionation occurred in the Elkhorn Mountains Volcanics, as only the most primitive lavas can be shown to have fractionated a small amount of ferromagnesian minerals and the ash-flow sheets only negligible amounts of plagioclase. Considering that the Elkhorn Mountains Volcanics and the Boulder batholith preserve different kinds of records (that is, the Elkhorn Mountains Volcanics preserve a record of the magma, whereas the Boulder batholith preserves crystallized products), such contrasts are predictable.

The Elkhorn Mountains Volcanics bear chemical characteristics similar to those of volcanics produced in modern subduction zone environments. The relatively constant REE abundances, with variable LREE enrichment, in the Elkhorn Mountains Volcanics (Figure 10) is typical of calc-alkaline volcanics in modern subduction zone environments (Condie, 1982), for example. The ranges of Rb (approximately 35-165 ppm) and Sr (approximately 300-1200 ppm) in the Elkhorn Mountains Volcanics (Tables 2 and 3; Figure 8) can be interpreted as indicating a source region in crust of 20-30 (or more) km thickness (Condie, 1973); calc-alkaline rocks generally are found on crust of comparable thickness over subduction zones of intermediate depth (100-200 km) (Condie, 1982).

The Zr abundances in the volcanic rocks and the experimental data of Watson (1979) regarding Zr and the $(Na_2O + K_2O)/Al_2O_3$ ratio of the liquid which can be interpreted as indicating that the parent magma of the Elkhorn Mountains Volcanics was peralkaline, may also reflect the depth to the source area. Increasing K_2O abundances in subduction-zone related volcanic rocks appear to correlate positively with the depth to the subduction zone (Hatherton and Dickinson, 1969; Dickinson, 1970).

Based on the peralkalinity of the magma and the intermediate crustal thickness and depth to the subduction zone inferred from the Rb and Sr abundances, it is likely that the source region of the Elkhorn Mountains Volcanics was more toward the continental interior than are the sources of many other subduction-related magmas (Hatherton and Dickinson, 1969; Dickinson, 1970).

From the overlapping igneous and tectonic activity (Robinson and others, 1968) and from the compressional nature of the deformation in the Elkhorn Mountains Volcanics -Boulder batholith region (Schmidt and Hendrix, 1981), it is clear that the volcanic and plutonic activity took place within a compressional framework, which, in terms of plate tectonics, is consistent with a subduction zone environment for the Late Cretaceous igneous activity in southwestern Montana. Although studies to date of the tectonic setting do not provide unequivocal evidence of a Late Cretaceous subduction zone to the west, the fact that the chemical characteristics of the Elkhorn Mountains Volcanics are similar to those of modern subduction zone calc-alkaline volcanics is consistent with such a tectonic environment.

The source region of the parent magma of the Elkhorn Mountains Volcanics and the Boulder batholith was probably the lower crust or upper mantle, based on the isotope variations in the plutonic rocks (Doe and others, 1968). Such a source region is consistent with the lack of a significant Eu anomaly in the volcanic

rocks, which implies that the source region of the Elkhorn Mountains Volcanics was not in the stability range of feldspar. If feldspar had been stable in the source, large Eu anomalies would be found, unless large amounts of melting occurred.

Because shallow level processes, such as crystal fractionation and magma mixing, have been rejected as dominant processes in the development of the Elkhorn Mountains Volcanics, an alternative origin of the chemical trends in the magmas must be considered. The major chemical characteristics of the magma could reflect the processes that occurred during the generation of the magma, probably by partial melting of a lower crustal or upper mantle source, instead of evolution in shallow-level magma chambers. This possibility is suggested as the explanation for both the "monotony" of the geochemistry of the Elkhorn Mountains Volcanics and similar eruptive units (see Figure 15) and their intermediate SiO_2 ranges.

APPENDIX

APPENDIX: CHEMICAL ANALYSES OF ASH-FALL SAMPLES

Sample Number	7	12	6	4	36	33	9	14	3	2
Major elements[1], weight %										
SiO_2	60.3	64.0	64.6	63.3	63.8	56.1	62.1	63.6	66.3	64.6
Al_2O_3	17.0	17.4	17.2	16.7	17.7	16.1	18.0	19.9	15.4	20.0
Fe_2O_3	5.2	2.7	3.3	4.3	3.2	5.7	4.4	1.6	3.5	1.5
FeO	2.7	2.6	3.0	2.9	3.1	4.8	3.5	2.2	1.8	4.0
MgO	2.7	1.4	1.4	2.1	3.1	4.8	2.1	.9	1.8	1.2
CaO	6.1	3.7	3.0	4.5	4.1	7.9	3.7	2.6	3.1	3.5
Na_2O	3.3	3.2	2.1	3.7	1.6	1.0	2.6	3.9	1.9	2.1
K_2O	1.1	3.6	4.2	1.2	2.1	1.9	2.4	4.2	4.8	2.0
TiO_2	.81	.87	.99	.89	.86	1.2	.90	.75	.82	.80
P_2O_5	.48	.35	.14	.15	.28	.30	.16	.23	.16	.21
MnO	.17	.10	.15	.09	.13	.27	.08	.12	.23	.04
Trace elements[2], ppm										
Ba	412	1200	1690	745	1090	761	1190	1130	1280	770
Co	16.1	10.6	10.6	14.7	14.0	25.7	19.3	7.1	10.2	8.1
Cr	11.3	9.9	22.1	24.0	25.4	59.0	42.7	3.0	37.1	26.6
Cs	1.1	2.5	4.0	.5	1.0	1.2	9.5	1.5	1.2	4.8
Cu	97	26	29	18	15	23	55	16	40	21
Hf	3.5	2.6	4.9	3.7	4.8	2.5	4.7	7.5	4.1	4.8
Ni	9	8	20	10	6	15	37	n.d.	41	9
Rb	31	104	115	128	49	42	101	93	105	64
Sb	.9	.2	.4	.2	.3	.3	.7	.3	.4	.3
Sc	10.7	11.8	14.0	15.6	15.8	28.0	17.5	11.5	10.6	18.7
Sr	730	650	640	500	610	590	660	550	580	780
Ta	.6	.9	.8	.6	.7	.4	.8	1.2	.6	.8
Th	4.4	11.5	9.9	5.7	8.8	4.1	9.6	15.0	6.7	7.8
U	1.0	2.4	1.7	1.4	2.2	1.2	1.4	3.5	1.7	.7
V	140	140	150	170	200	350	200	80	100	230
Y	18	24	20	20	20	18	18	28	17	17
Zn	122	86	79	76	81	132	82	83	69	77
Zr	190	410	210	170	210	240	260	410	140	360
La	34.1	49.1	42.0	29.7	38.7	25.5	38.2	63.7	29.7	30.8
Ce	60	86	78	53	70	47	68	11.3	53	55
Sm	5.3	7.3	6.3	5.1	6.3	5.1	6.0	9.5	4.9	5.1
Eu	1.43	1.85	1.54	1.31	1.56	1.29	1.53	2.39	1.27	1.44
Tb	.61	.90	.68	.56	.76	.59	.66	1.19	.55	.62
Yb	1.9	2.7	2.0	2.1	2.3	1.8	1.9	3.3	1.9	1.9
Lu	.31	.39	.32	.31	.35	.29	.30	.50	.30	.31

Analyses normalized to 100% anhydrous.
1 = All major elements by ICP except FeO by titration and TiO_2 and P_2O_5 colorimetrically (U.S. Geological Survey, J. Gillison, Analyst).
2 = All trace elements by INAA (U.S. Geological Survey, G. A. Wandless, Analyst), except Cu by flame atomic absorption, Ni and V by graphite furnace atomic absorption, and Sr, Y, and Zr by ICP (U.S. Geological Survey, W. D'Angelo, Analyst).

REFERENCES

Abbey, S., 1978, U.S.G.S. II revisited: Geostandards Newsletter, v. 2, p. 141-146.

Abbey, S., 1983, Studies in "standard samples" of silicate rocks and minerals 1969-1982: Geol. Surv. Canada Paper 83-15, 114p.

Arth, J., 1976, Behavior of trace elements during magmatic processes - A summary of theoretical models and their applications: Jour. Research U.S. Geol. Survey, v. 4, p. 41-47.

Bacon, C. R., McDonald, R., Smith, R. L., and Baedecker, P. A., 1981, Pleistocene high-silica rhyolites of the Coso volcanic field, Inyo, California: Jour. Geophys. Res., v. 86, p. 10223-10241.

Baker, B. H., and McBirney, A. R., 1985, Liquid fractionation. Part III: Geochemistry of zoned magmas and the compositional effects of liquid fractionation: Jour. Volcan. Geoth. Res., v. 24. p. 55-81.

Becraft, G. E., Pinckney, D. M., and Rosenblum, S., 1963, Geology and mineral deposits of the Jefferson City quadrangle, Jefferson and Lewis and Clark counties, Montana: U.S. Geol. Surv. Prof. Paper 428, 101p.

Blake, S., 1981, Eruptions from zoned magma chambers: Jour. Geol. Soc. London, v. 138, p. 281-287.

Byers, F. M., Jr., Carr, W. J., Orkild, P. P., Quinlivan, W. D., and Sargent, K. A., 1976, Volcanic suites and related cauldrons of Timber Mountain-Oasis Valley caldera complex, southern Nevada: U.S. Geological Survey Prof. Paper 919, 70p.

Cameron, K. L., 1983, The Bishop Tuff revisited: Isotope dilution REE data consistent with crystal fractionation: EOS Transactions AGU, v. 64, p. 883.

Carr, W. J., Byers, F. M., Jr., and Orkild, P. P., 1984, Stratigraphic and volcano-tectonic relations of Crater Flat Tuff and some older volcanic units, Nye County, Nevada: U.S. Geol. Surv. Open-file Rept. 84-114.

Christiansen, R. L., 1979, Cooling units and composite sheets in relation to caldera structure, in Chapin, C. E., and Elston, W. E., eds., Ash-flow tuffs: Geol. Soc. Amer. Spec. Paper 180, p. 29-42.

Christiansen, R. L., Lipman, P. W., Carr, W. J., Byers, F. M., Jr. Orkild, P. P., and Sargent, K. A., 1977, Timber Mountain-Oasis Valley Caldera complex of southern Nevada: Geol. Soc. Amer. Bull., v. 88, p. 943-959.

Condie, K. C., 1973, Archean magmatism and crustal thickening: Geol. Soc. Amer. Bull., v. 84, p. 2981-1992.

Condie, K. C., 1982, Plate tectonics and crustal evolution, 2nd ed.: Pergamon, New York, 310p.

Cox, K. G., 1980, A model for flood basalt volcanism: Jour. Petrol., v. 21, p. 629-650.

Cox, K. G., Bell, J. D., and Pankhurst, R. J., 1979, The Interpretation of Igneous Rocks: George Allen and Unwin, London, 450p.

Dickinson, W. R., 1970, Relations of andesites, granites, and derivative sandstones to arctrench tectonics: Rev. Geophys. Space Phys., v. 8, p. 813-860.

Doe, B. R., Tilling, R. I., Hedge, C. E., and Klepper, M. R., 1968, Lead and strontium isotope studies of the Boulder batholith, southwestern Montana: Econ. Geol., v. 63, p. 884-906.

Flanagan, F. J., ed., 1976, Description and analyses of eight new U.S.G.S. rock standards: U.S. Geol. Surv. Prof. Paper 840, 192p.

Freeman, V. L., Ruppel, E. T., and Klepper, M. R., 1958, Geology of part of the Townsend Valley, Broadwater and Jefferson counties, Montana: U.S. Geol. Surv. Bull. 1042-N.

Gill, J. B., 1978, Partition coefficients in models of andesite genesis: Geochim. et Cosmochim. Acta, v. 42, p. 709-724.

Hamilton, W., and Myers, W. B., 1974, Nature of the Boulder batholith of Montana: Geol. Soc. Amer. Bull., v. 85, p. 365-378.

Haskin, L. A., Haskin, M. A., Frey, F. A., and Wildeman, T. R., 1968, Relative and absolute terrestrial abundances of the rare earths, in L. H. Ahrens, ed., Origin and distribution of the elements: Pergamon Press, New York, p. 889-912.

Hatherton, T., and Dickinson, W. R., 1969, The relationship between andesitic volcanism and seismicity in Indonesia, the Lesser Antilles, and other island arcs: Jour. Geophys. Res., v. 74, p. 5301-5310.

Hildreth, W., 1979, The Bishop Tuff: Evidence for the origin of compositional zonation in silicic magma chambers, in Chapin, C. E., and Elston, W. E., eds., Ash-flow tuffs: Geol. Soc. Amer. Spec. Paper 180, p. 43-75.

Hildreth, W., 1981, Gradients in silicic magma chambers: Implications for lithospheric magmatism: Jour. Geophys. Res., v. 86, p. 10153-10192.

Huppert, H. E., and Sparks, R. S. J., 1984, Double-diffusive convection due to crystallization in magmas: Ann. Rev. Earth Planet. Sci., v. 12, p. 11-37.

Hyndman, D. W., Talbot, J. L., and Chase, R. R., 1975, Boulder batholith: A result of emplacement of a block detached from the Idaho batholith infrastructure: Geology, v. 3, p. 401-404.

Klepper, M. R., and Smedes, H. W., 1959, Elkhorn Mountains volcanic field, western Montana (abst.): Geol. Soc. Amer. Bull., v. 70, p. 1631.

Klepper, M. R., Weeks, R. A., Ruppel, E. T., 1957, Geology of the southern Elkhorn Mountains, Jefferson and Broadwater counties, Montana: U.S. Geol. Surv. Prof. Paper 292, 82p.

Klepper, M. R., Robinson, G. D., and Smedes, H. W., 1971, On the nature of the Boulder batholith of Montana: Geol. Soc. Amer. Bull., v. 82, p. 1563-1580.

Klepper, M. R., Ruppel, E. T., Freeman, V. L., and Weeks, R. A., 1971, Geology and mineral deposits, east flank of the Elkhorn Mountains, Broadwater County, Montana: U.S. Geol. Surv. Prof. Paper 665, 66p.

Knopf, A., 1957, The Boulder batholith of Montana: Amer. Jour. Sci., v. 255, p. 81-103.

Knopf, A., 1963, Geology of the northern part of the Boulder bathylith and adjacent area, Montana: U.S. Geol. Surv. Map I-381.

Lambe, R. N., 1981, Crystallization and petrogenesis of the southern portion of the Boulder batholith, Montana: Unpublished Ph.D. dissertation, Berkeley, University of California, 171p.

Leat, P. T., McDonald, R., and Smith, R. L., 1984, Geochemical evolution of the Menengai Caldera Volcano, Kenya: Jour. Geophys. Res., v. 89, p. 8571-8592.

Lipman, P. W., 1965, Chemical comparison of glassy and crystalline volcanic rocks: U.S. Geol. Surv. Bull. 1201-D, p. D1-D23.

Lipman, P. W., 1979, Emplacement of high-level granitic batholiths: Evidence from the San Juan volcanic field of Colorado and the Boulder batholith of Montana: Geol. Soc. Amer., Abst. w/Programs, v. 11, p. 467.

Lipman, P. W., 1984, The roots of ash flow calderas in western North America: Windows into the tops of granitic batholiths: Jour. Geophys. Res., v. 89, p. 8801-8841.

Lipman, P. W., Christiansen, R. L., and O'Connor, J. T., 1966, A compositionally zoned ash-flow sheet in southern Nevada: U.S. Geol. Surv. Prof. Paper 524-5, 46p.

Mahood, G. A., 1981, A summary of the geology and petrology of the Sierra La Primavera, Jalisco, Mexico: Jour. Geophys. Res., v. 86, p. 10137-10152.

Marsh, B. D., 1981, On the crystallinity, probability of occurrence, and rheology of lava and magma: Contrib. Mineral. Petrol., v. 78, p. 85-95.

Michael, P. J., 1983, Chemical differentiation of the Bishop Tuff and other high-silica magmas through crystallization processes: Geology, v. 11, p. 31-34.

Miyashiro, A., 1974, Volcanic rock series in island arcs and active continental margins: Amer. Jour. Sci., v. 274, p. 321-355.

Mutschler, F. E., Rougon, D. J., and Lavin, O. P., 1976a, PETROS - a data bank of major-element chemical analyses of igneous rocks for research and teaching: Comput. Geosci., v. 2, p. 51-57.

Mutschler, F. W., Rougon, D. J., and Lavin, O. P., 1976b, PETROS - a data bank of major-element chemical analyses of igneous rocks for reserach and teaching: Comput. Geosci., v. 2, p. 51-57.

Nelson, W. H., 1963, Geology of the Duck Creek Pass quadrangle, Montana: U.S. Geol. Surv. Bull. 1121-J.

Noble, D. C., 1967, Sodium, potassium, and ferrous iron contents of some secondarily hydrated natural silicic glasses: Amer. Mineral., v. 52, p. 280-286.

Robinson, G. D., 1963, Geology of the Three Forks quadrangle, Montana, with descriptions of igneous rocks by H. Frank Barnett: U.S. Geol. Surv. Prof. Paper 370, 143p.

Robinson, G. D., and Marvin, R. F., 1967, Upper Cretaceous volcanic glass from western Montana: Geol. Soc. Amer. Bull., v. 78, p. 601-608.

Robinson, G. D., Klepper, M. R., and Obradovich, J. D., 1968, Overlapping plutonism, volcanism, and tectonism in the Boulder batholith region, western Montana: Geol. Soc. Amer. Mem. 116, p. 557-576.

Rosholt, J. N., and Noble, D. C., 1969, Loss of uranium from crystallized silicic volcanic rocks: Earth Planet. Sci. Lett., v. 6, p. 268-270.

Rosholt, J. N., Prijana, and Noble, D. C., 1971, Mobility of uranium and thorium in glassy and crystallized silicic volcanic rocks: Econ. Geol., v. 66, p. 1061-1069.

Ross, C. S., and Smith, R. L., 1961, Ash-flow tuffs: Their origin, geologic relations and identification: U.S. Geol. Surv. Prof. Paper 336, 54p.

Ruppel, E. T., 1961, Reconnaissance geologic map of the Deer Lodge quadrangle, Powell, Deer Lodge and Jefferson counties, Montana: Map MF 174.

Ruppel, E. T., 1963, Geology of the Basin quadrangle, Jefferson, Lewis and Clark, and Powell counties, Montana: U.S. Geol. Surv. Bull. 151, 121p.

Schmidt, C. J., and Hendrix, T. E., 1981, Tectonic controls for thrust belt and Rocky Mountain foreland structures in the northern Tobacco Root Mountains - Jefferson Canyon area, southwestern Montana: Montana Geol. Soc., 1981 Field Conf. Guidebook, p. 167-180.

Scott, R. B., Byers, F. M., and Warren, R. G., 1984, Evolution of magma below clustered calderas, southwest Nevada volcanic field: EOS Trans. AGU, v. 65, p. 1126-1127.

Smedes, H. W., 1962, Preliminary geologic map of the northern Elkhorn Mountains, Jefferson and Broadwater counties, Montana: U.S. Geol. Surv. Map MF-243.

Smedes, H. W., 1966, Geology and igneous petrology of the northern Elkhorn Mountains, Jefferson and Broadwater counties, Montana: U.S. Geol. Surv. Prof. Paper 510, 116p.

Smedes, H. W., 1967, Preliminary geologic map of the Butte South quadrangle, Montana: U.S. Geol. Surv. Open-File Rept.

Smedes, H. W., Klepper, M. R., Pinckney, D. M., Becraft, G. E., and Ruppel, E. T., 1962, Preliminary geologic map of the Elk Park quadrangle, Jefferson and Silver Bow counties, Montana: U.S. Geol. Surv. Map MF-246.

Smith, R. L., 1960a, Ash flows: Geol. Soc. Amer. Bull., v. 71, p. 795-842.

Smith, R. L., 1979, Ash-flow magmatism, in Chapin, C. E., and Elston, W. E., eds., Ash-flow tuffs: Geol. Soc. Amer. Spec. Paper 180, p. 5-27.

Smith, R. L., and Bailey, R. A., 1966, The Bandelier Tuff: A study of ash-flow eruption cycles from zoned magma chambers: Bull. Volcanologique, v. 29, p. 83-104.

Spera, F. J., 1984, Some numerical experiments on the withdrawal of magma from crustal reservoirs: Jour. Geophys. Res., v. 89, p. 8222-8236.

Steven, T. A., and Lipman, P. W., 1976, Calderas of the San Juan volcanic field, southwestern Colorado: U.S. Geol. Surv. Prof. Paper 958, 35p.

Taylor, S. R., 1969, Trace element chemistry of andesites and associated calc-alkaline rocks, in McBirney, A. R., ed., Proc. Andesites Conf.: Dept. Geol. Min. Res. Oregon Bull., v. 65, p. 43-64.

Tilling, R. I., 1973, Boulder batholith, Montana: A product of two contemporaneous but chemically distinct magma series: Geol. Soc. Amer. Bull., v. 84, p. 3879-3900.

Tilling, R. I., 1974, Composition and time relations of plutonic and associated volcanic rocks, Boulder batholith region, Montana: Geol. Soc. Amer. Bull., v. 85, p. 1925-1930.

Tilling, R. I., 1977, Interaction of meteoric waters with magmas of the Boulder batholith, Montana: Economic Geoogy, v. 72, p. 859-864.

Tilling, R. I., Klepper, M. R., and Obradovich, J. D., 1968, K-Ar ages and time span of emplacement of the Boulder batholith, Montana: Amer. Jour. Sci., v. 266, p. 671-689.

U.S. Geol. Survey and U.S. Bureau of Mines (Greenwood, W. R.), 1978, Mineral resources of the Elkhorn Wilderness study area, Montana: U.S. Geol. Surv. Open-File Rept. 78-325.

Watson, E. B., 1979, Zircon saturation in felsic liquids: Experimental results and applications to trace element geochemistry: Contrib. Mineral. Petrol., v. 70, p. 407-419.

Whitney, J. A., and Stormer, J. C., Jr., 1985, Mineralogy, petrology, and magmatic conditions from the Fish Canyon Tuff, central San Juan volcanic field, Colorado: Jour. Petrology, v. 26, p. 726-762.

Williams, H., 1941, Calderas and their origin: California Univ. Pub., Dept. Geol. Sci. Bull., v. 25, no. 6, p. 239-346.